

1-1-2019

Production and ecosystem structure in cold-core vs. warm-core eddies: Implications for the zooplankton isoscape and rock lobster larvae

Anya M. Waite

Eric Raes

Lynnath E. Beckley

Peter A. Thompson

David Griffin

See next page for additional authors

Follow this and additional works at: <https://ro.ecu.edu.au/ecuworkspost2013>



Part of the [Ecology and Evolutionary Biology Commons](#)

[10.1002/Ino.11192](https://ro.ecu.edu.au/ecuworkspost2013/7184)

Waite, A. M., Raes, E., Beckley, L. E., Thompson, P. A., Griffin, D., Saunders, M., ... Jeffs, A. (2019). Production and ecosystem structure in cold-core vs. warm-core eddies: Implications for the zooplankton isoscape and rock lobster larvae. *Limnology and Oceanography*, 64(6), 2405-2423. Available [here](#)


This Journal Article is posted at Research Online.

<https://ro.ecu.edu.au/ecuworkspost2013/7184>

Authors

Anya M. Waite, Eric Raes, Lynnath E. Beckley, Peter A. Thompson, David Griffin, Megan Saunders, Christin Sawstrom, Richard O'Rourke, Miao Wang, Jason P. Landrum, and Andrew Jeffs

Production and ecosystem structure in cold-core vs. warm-core eddies: Implications for the zooplankton isoscape and rock lobster larvae

Anya M. Waite ^{1,2,3*} Eric Raes ^{2,4} Lynnath E. Beckley,⁵ Peter A. Thompson,⁴ David Griffin,⁴ Megan Saunders,⁶ Christin Sävström,⁷ Richard O'Rorke ⁸ Miao Wang,⁹ Jason P. Landrum,¹⁰ Andrew Jeffs⁸

¹School of Civil, Environmental and Mining Engineering and The Oceans Institute, The University of Western Australia, Crawley, Western Australia, Australia

²Alfred Wegener Institute, Helmholtz Centre for Polar and Marine Research, Universität Bremen, Bremen, Germany

³Ocean Frontier Institute and Department of Oceanography, Dalhousie University, 1355 Oxford St., Halifax, Nova Scotia, Canada

⁴CSIRO Oceans and Atmosphere, Hobart, Tasmania, Australia

⁵Environmental and Conservation Sciences, Murdoch University, Murdoch, Western Australia, Australia

⁶School of Chemical Engineering, The University of Queensland, St Lucia, Queensland, Australia

⁷School of Science, Centre for Marine Ecosystems Research (CMER), Edith Cowan University, Joondalup, Western Australia, Australia

⁸Institute of Marine Science, University of Auckland, Auckland, New Zealand

⁹Key Laboratory of Tropical & Subtropical Fishery Resource Application & Cultivation, Pearl River Fisheries Research Institute, Chinese Academy of Fishery Science, Guangzhou, China

¹⁰Lenfest Ocean Program, The Pew Charitable Trusts, Washington, District of Columbia

Abstract

Anticyclonic (warm-core) mesoscale eddies (WCEs) in the Eastern Indian Ocean carry higher surface chlorophyll signatures than cyclonic (cold-core) eddies (CCEs). Paradoxically, WCEs host rock lobster larvae (phyllosomas) with lower lipid stores and protein reserves than phyllosomas in CCEs, suggesting a poorer nutritional status. We assess primary productivity and zooplankton isotopic data from eight eddies across four research voyages (2003–2011) to determine how this contradiction might occur. We find that WCEs and CCEs are equally productive per unit chlorophyll *a*, but depth-integrated primary production (PP) is greater in eddies with shallower mixed layers (MLs), especially in CCEs. MLs tend to be shallower in CCEs than in WCEs because the pycnocline is closer to the surface. This, in combination with stronger stratification in CCE euphotic zones than those of WCEs, supports greater flagellate and dinoflagellate populations in CCEs. These phytoplankton provide high-quality nutrition for zooplankton, which feed on average ~0.6 trophic level lower in CCEs with the shallowest MLs, accumulating high lipid stores. Conversely, WCEs have, on average, ~70 m deeper MLs than CCEs, and host a phytoplankton community with more diatoms. Diatoms provide lower quality food for zooplankton, and zooplankton lipid stores in WCEs decline with trophic level, and possibly, with time after initial (or seasonal) nutrient injection. As a result, phyllosomas in CCEs have higher energy and lipid content than those in warm-core eddies. The resolution of the paradox, therefore, is that the higher surface chlorophyll signatures of WCEs are not representative of the nutritional value of the prey field of the phyllosoma. We also conclude that interannual variations of mixed layer depth occur at a regional scale, controlling PP.

Large mesoscale eddies in oligotrophic regions can significantly impact productivity (Chelton et al. 2011). The eddies generated by the Leeuwin Current (LC) in the eastern Indian Ocean

transport nutrients into surface waters, either by moving nutrients offshore from the coast (anticyclonic warm-core eddies [WCEs]) or by lifting nutrients from deeper waters (cyclonic cold-core eddies [CCEs]) (Cresswell and Griffin 2004). In this system, WCEs tend to have a deep surface ML with well-mixed and relatively high chlorophyll *a* (Chl *a*) concentrations (Waite et al. 2007a). In contrast, the pycnoclines of CCEs are often more physically stratified than WCEs, limiting significant nutrient flux and chlorophyll accumulation to a (relatively) small

*Correspondence: anya.waite@dal.ca

This is an open access article under the terms of the Creative Commons Attribution License, which permits use, distribution and reproduction in any medium, provided the original work is properly cited.

depth range near the pycnocline. Here, nutrients are made available through pycnocline elevation (Greenwood et al. 2007; Waite et al. 2007b) and through isopycnal mixing (Pidcock et al. 2016). Evidence of higher chlorophyll concentrations in WCEs determined from remote sensing has suggested that WCEs are generally more productive, driven both by incorporation of nutrients from the coast (Paterson et al. 2008) and by the seasonal injection of deep nutrients across the pycnocline in the Indian Ocean (Dufois et al. 2016). WCEs also have higher N_2 fixation rates (Raes et al. 2015), greater depth-integrated Chl *a*, and depth-integrated primary production (PP) than CCEs, as well as a greater proportion of diatoms in their phytoplankton biomass (Thompson et al. 2007; Waite et al. 2007b).

However, detailed examination in the south-east Indian Ocean has shown that CCEs can sometimes be more productive per unit Chl *a* than WCEs, because CCEs have more actively dividing populations of small phytoplankton including nanoplankton and picoplankton (Thompson et al. 2007). CCEs also support relatively more abundant populations of dinoflagellates, including heterotrophic dinoflagellates such as *Protoperdinium* spp., such that their ecosystems are actually more heterotrophic than those of WCEs (Waite et al. 2007a). This positive covariation of productivity and heterotrophy is in strong contrast to classical spring bloom dynamics in higher latitudes, where diatom blooms are both more autotrophic and more productive, than dinoflagellate growth (e.g., Waite et al. 1992; Höglander et al. 2004). Thus, ecosystems supported by CCEs may have the same close coupling of autotrophy and heterotrophy suggested by Behrenfeld (2010) for the North Atlantic Ocean. Higher Chl *a*-specific productivity, at lower Chl *a* concentrations, also suggests the possibility for top-down (grazer) control of biomass in CCEs. However, it is unclear whether this is generally true for all CCEs, and these ideas remain to be tested.

The LC system itself is an anomalous boundary current, which does not follow a typical seasonal cycle in mixed layer depth (MLD) due to unusually strong regional salinity stratification, with isotherms that tilt downward toward the Australian coast (Feng et al. 2003). A strong pycnocline, associated with a deep chlorophyll maximum (DCM), may be a ubiquitous and year-round feature (Hanson et al. 2007), other than a short period in late autumn (Rousseaux et al. 2012), leading to chronic nutrient limitation of surface ecosystems (Hanson et al. 2005; Raes et al. 2015).

A very sparse and poor-quality prey field in the south-eastern Indian Ocean suggests that rock lobster phyllosoma larvae are endemically food-limited (Säwström et al. 2014). During the important winter period prior to their shoreward migration, the LC is a good source of their preferred prey during the autumn/winter phytoplankton bloom (Säwström et al. 2014). However, phyllosomas are not usually found within the LC at this time, as most phyllosomas remain offshore and further south, in cooler and (at this time) less nutrient-rich subtropical waters (STW). There are a number of possible explanations for this spatial mismatch of

phyllosomas and their prey, including an improved availability or quality of food in STW (Wang et al. 2014a,b, 2015), offshore reduction in predation on evolutionary time scales (Wasmund et al. 2001; Säwström et al. 2014), or improved opportunity to be transported or recruited to more desirable locations on the coast (Caputi 2008).

We recently showed that phyllosomas found in both WCEs and CCEs consumed a diverse diet of colonial radiolaria, larval fishes, hydrozoans, (particularly siphonophores), scyphozoans, salps, chaetognaths, and krill (O'Rourke et al. 2015; Wang et al. 2015). However, late stage phyllosomas caught feeding in CCEs were significantly richer in lipid and protein than those from WCEs (Wang et al. 2015). Together, these studies leave the question unanswered as to why phyllosomas feeding in CCEs are in much better nutritional condition than their WCE counterparts (Wang et al. 2014b; O'Rourke et al. 2015) even though surface Chl *a* concentrations are higher in WCEs.

In this article, we test the hypothesis that CCEs are actually more productive than their visible surface Chl *a* signature suggests, and more productive overall than WCEs. If the productive layer of CCEs is trapped within the pycnocline and not clearly visible from satellite observations, the better nutritional condition of the phyllosomas in CCEs could simply be driven bottom up, via higher primary productivity in CCEs supporting lipid-rich zooplankton feeding on dinoflagellates.

Materials and methods

On the RV *Southern Surveyor* (2003–2011), we sampled phyllosoma in eight eddies (two in 2003; one in 2006; five in 2011) across the two primary regional water masses in our southeast Indian Ocean study region (Fig. 1A), which we surveyed regionally with transects in 2010 (28–34°S and 110–116°E; Fig. 2D,E; Table 1): The primary water masses sampled were the LC, a warm shelf-break boundary current flowing southward centered along the 200 m depth contour, and the cooler STW seaward of the LC. Our analyses here include both unpublished data (2010–2011) and earlier published data from the voyage in October 2003 (Waite et al. 2007a,b; Paterson et al. 2008).

In 2003, two large eddies were identified as major positive (WCE) and negative (CCE) sea-surface height anomalies (SSHAs) (Fig. 1C–F). In October 2003, at the time of sampling, these were approximately 5 months old (Feng et al. 2007). While each eddy was sampled up to 50 times over a 3-week period (Fig. 1B; Waite et al. 2007a), for the purpose of this study, we selected stations with PP measurements in the central core of the eddies (Fig. 1C,D), where productivity was unlikely to be impacted by complex processes occurring at eddy boundaries (Omand et al. 2015). For the 2003 WC Eddy (WC03), this narrowed the field to six stations within a 60 km radius from the eddy center (Fig. 1C), while for the CC eddy (CC03), a smaller feature, we selected four stations within 30 km of the eddy center (Fig. 1D). These two features have been well studied (12 papers in a special issue of Deep-Sea Research II (Vol 54 [8–10]; 2007)

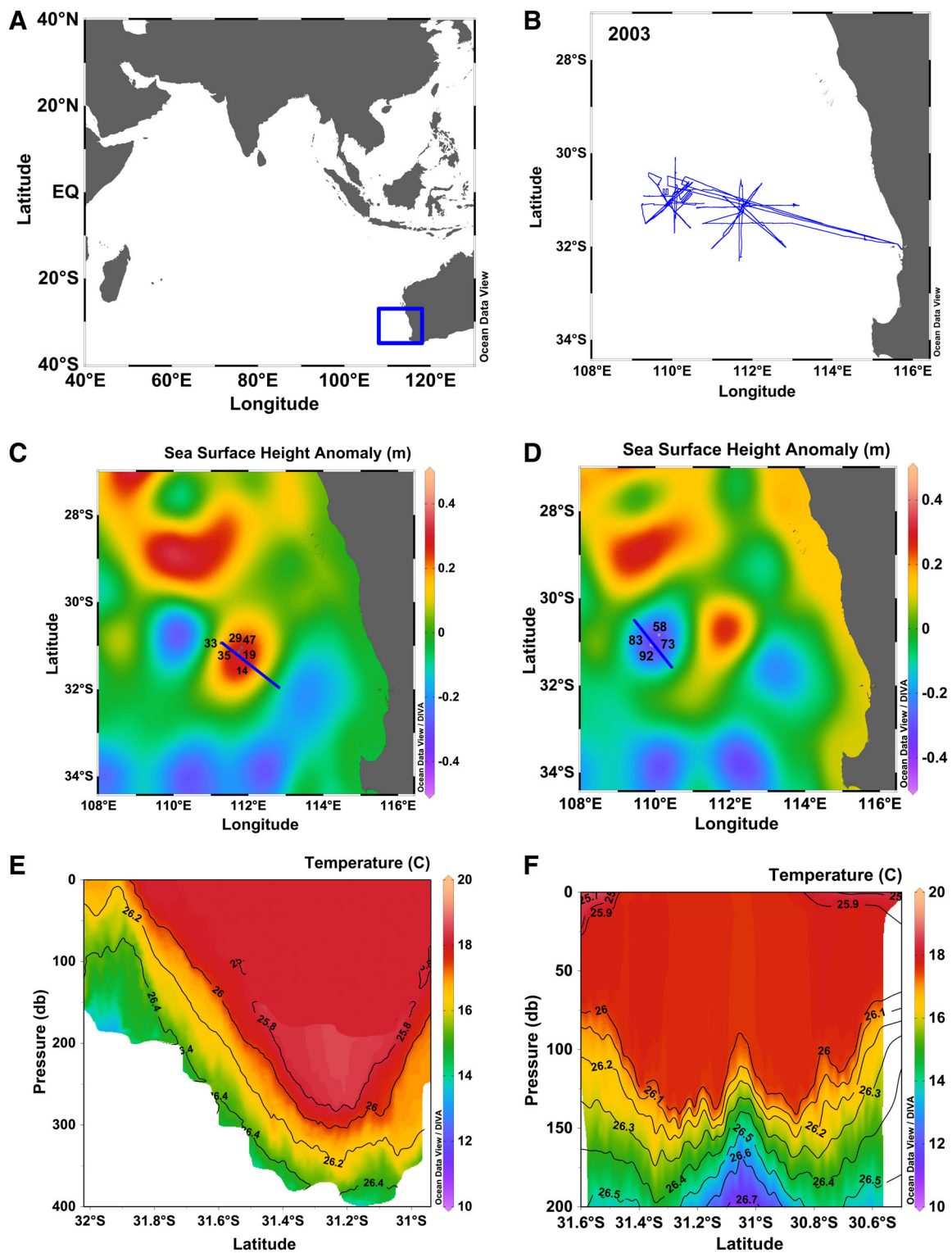


Fig. 1. Map, ship track and cross-sections of the WCE and CCE sampled in 2003. **(A)** Regional map with the 2003 study area as a rectangle. **(B)** Ship track in 2003 showing the survey of one WCE and one CCE (see Waite et al. 2007a). **(C)** SSHA for 04 October 2003 showing the WCE as positive SSHA (WC03) with station and transect locations (02–09 October). **(D)** As for C, but showing station and transect locations of the CCE (CC03) for 13 October 2003. **(E)** Transect through WC03 showing temperature in color, with density contours as black lines. **(F)** As for E, but showing transect for CCE (CC03).

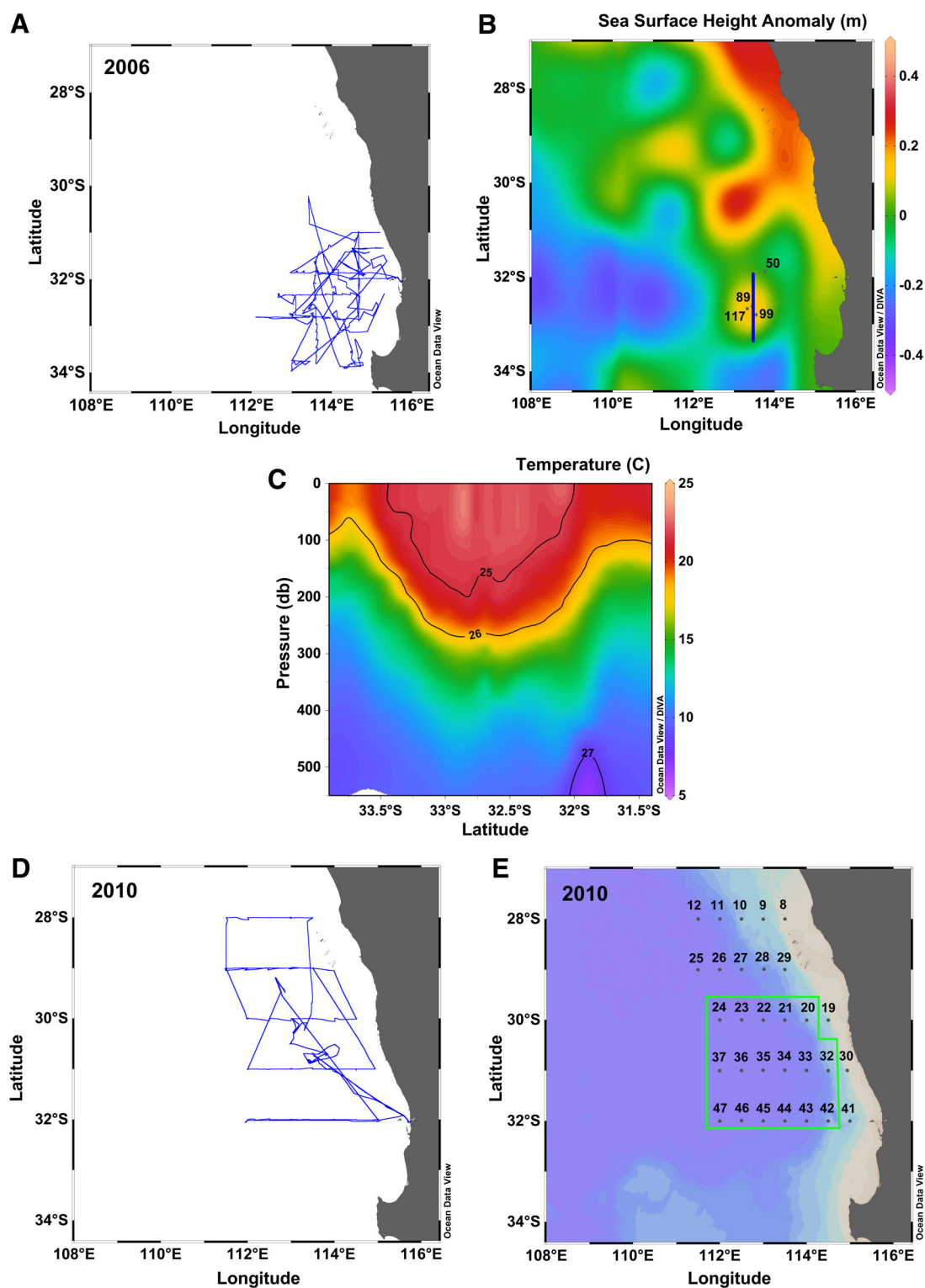


Fig. 2. Ship track and cross-sections of WCEs and CCEs sampled in 2006, and regional sampling in 2010. **(A)** Ship track in 2006 showing survey of one forming mesoscale eddy (see Paterson et al. 2008). **(B)** SSHA for 25 May 2006 showing a WCE as positive SSH (WC06) with station and transect locations. **(C)** Transect through WC06 with temperature as color and density as black contours. **(D)** Map and ship track of the 2010 research voyage, which was a regional survey for zooplankton and phyllosoma sampling (no eddies targeted). **(E)** Stations west and south of the Leeuwin Current. Source: Säwström et al. (2014).

Table 1. Synthesis of phytoplankton data from eight mesoscale eddies (four WCEs: WC03, WC06, WC11A, WC11B, and four CCEs: CC03, CC11a, C11b, C11c); see Figs. 1–3 for all eddy locations and CTD station locations. ND indicates no data available.

CTD	Distance from Ctr (km)	MLD (m)	Integrated Chl <i>a</i> (to 150 m)	Integrated PP (mg m ⁻² d ⁻¹)	%diatoms (%count)	%dinoflagellates (%count)	%DVChl <i>a</i> (%Chl <i>a</i>)	%Fuco (%Chl <i>a</i>)	%Diadeno (%Chl <i>a</i>)
WCEs									
WC03									
35	8	278	32	450.7	41.8	3.6	0	14.0	15.9
19	10	272	35	634.4	38.2	5.5	0	18.0	11.2
14	14	280	39	461.8	27.3	9.1	0	23.9	4.8
47	15	276	73	722.5	27.3	10.6	0	10.0	7.8
29	18	275	52	275.4	18.2	5.5	0	15.5	8.0
33	57	111	33	263	25.5	12.7	13.0	7.4	9.1
WC03avg	20	249	44	468.0	29.7	7.8	2.2	14.8	9.5
STD		67	16	185.4	8.7	3.5	5.3	5.9	3.8
<i>n</i>		6	6	6	6	6	6	6	6
WC06									
50	88	82	38	4018	ND	ND	12.2	11.7	5.1
89	22	101	22	1784	ND	ND	12.6	5.0	3.7
99	16	117	37	3354	ND	ND	13.1	8.9	7.5
117	16	153	32	3422	ND	ND			
WC06avg	18	113	32	3144.5	ND	ND	12.6	8.5	5.4
STD			8.9	955			0.5	3.3	1.9
<i>n</i>			3	4			3	3	3
WC11A									
	Date								
4	26 Aug 2011	158	47.1	ND	ND	ND	13.8	6.3	4.0
10	30 Aug 2011	34	49.2	2391.5	20.1	73	4.8	6.8	6.8
WC11Aavg		96	48.2	2391.5	20.1	73.0	9.3	6.6	5.4
STD		88	1	ND	ND	ND	6	0	2
<i>n</i>		2	2	1	1	1	2	2	2
WC11Bavg									
8	28 Aug 2011	156	51.5	2454.9	15.4	78.9	1.8	8.2	6.4
All WCEs		153	43.9	2114.7	21.7	53.2	6.5	9.5	6.7
STD		68	8.5	1149.6	7.3	39.4	5.4	3.6	1.9
<i>n</i>		4	4	4	3	3	4	4	4
CCEs									
CC03									
83	8	107	15	211.6	5.5	5.5	33.0	10.5	7.4
73	10	118	21	133.7	10.9	14.5	27.3	0.0	3.7
92	14	117	17	181.2	0.0	10.9	40.6	0.0	4.2
58	28	141	26	99.5	7.3	18.2	33.7	0.0	4.5
CC03avg		121	20	156.5	5.9	12.3	33.6	2.6	4.9
STD		14	5	49.7	4.5	5.4	5.5	5.3	1.7
<i>n</i>		4	4	4	4	4	4	4	4
CC11a									
	Date								
3	25 Aug 2011	58	37.0	1499	8.8	81.2	ND	ND	ND
9	29 Aug 2011	72	46.2	1980	6.7	82.4	ND	ND	ND
CC11a avg		65	41.6	1739.5	7.8	81.8	ND	ND	ND
STD		10	6.5	340.1	1.5	0.8	ND	ND	ND
<i>n</i>		2	2	2	2	2	ND	ND	ND

(Continues)

Table 1. Continued

CTD	Distance from Ctr (km)	MLD (m)	Integrated Chl <i>a</i> (to 150 m)	Integrated PP (mg m ⁻² d ⁻¹)	%diatoms (%count)	%dinoflagellates (%count)	%DVChl <i>a</i> (%Chl <i>a</i>)	%Fuco (%Chl <i>a</i>)	%Diadeno (%Chl <i>a</i>)
CC11b									
7	27 Aug 2011	70	29.7	1574.1	5	75.5	25.8	6.7	5.6
12	31 Aug 2011	64	32.5	2103.9	6.6	83.8	25.7	5.7	2.9
19	05 Aug 2011	18	41.3	2518.1	ND	ND	0.0	19.5	5.3
20	05 Sep 2011	54	18.9	1152	ND				
CC11b avg		52	30.6	1837.0	5.8	79.7	17.2	10.7	4.6
STD		23	9.2	598.2	1.1	5.9	0.1	0.7	2.0
<i>n</i>		4	4	4	2	2	3	3	3
CC11c avg									
13	01 Sep 2011	102	32.3	1535.3	10.6	71.6	ND	ND	ND
All CCEs		85	31.1	1317.1	7.5	61.3	25.4	6.7	4.8
STD		32	8.9	783.9	2.2	33.0	11.6	5.7	0.3
<i>n</i>		4	4	4	4	4	2	2	2

Where eddies were sampled intensively, the distance from eddy center is provided for each CTD cast shown. Where eddies were sampled only 1–2 times (as close as possible to the eddy center), the date is given to indicate time between samples. Data in bold represent means of data for individual eddies.

so we will not describe them in detail here, but a subset of the conductivity-temperature-depth (CTD) data, including a single CTD transect through each feature, are shown for comparison with the other eddies (Fig. 1E,F). In 2006, we selected stations within 30 km of the eddy center (Fig. 2A,B). For all voyages described here, data are available online, e.g., https://www.cmar.csiro.au/data/rawler/survey_details.cfm?survey=SS200308. All satellite SSH (from altimetry) data are provided via the Integrated Marine Observing System database (IMOS; <http://oceancurrent.imos.org.au/sourcedata/>).

In 2010, no eddies were deliberately targeted, instead we executed a regional sampling effort across five E-W transects spaced 1° apart, from 28°S to 32°S, with stations spaced 0.5° (E) apart, to ~ 112°E (Sawström et al. 2014; Fig. 2D,E). We sampled zooplankton populations regionally during this voyage, from which abundance data were analyzed and presented by Sawström et al. (2014). Here, the data from the 2010 voyage that we present are the unpublished isotopic signatures of the selected and size-fractionated zooplankton (see below for sampling and analysis details).

In 2011, as part of a study targeting the phyllosoma larvae of the Western Rock Lobster *Panulirus cygnus*, we sampled five eddies identified by their SSHA (Fig. 3B,C); two WCEs (marked A and B; Fig. 3B–E) and three CCEs (marked a, b, and c, capitalization change intentional, see Fig. 3B,C,F–H) over 3 weeks. Other than the CCE c, which was sampled once, all eddies were sampled as close as possible to the eddy center, at least twice during the research voyage. Towed-CTD measurements were executed from near the center of each feature radially outward toward its perimeter (blue lines, Fig. 3B,C). The towed undulating CTD unit (Nacelle) was equipped with a Digiquartz pressure sensor, a Seabird SBE3plus temperature sensor, Seabird SBE4C conductivity

sensor, Ecotriplet fluorometer, and a dissolved oxygen sensor (Optode model 3975, on some deployments only).

For temperature and salinity measurements in situ, we used a Seabird SBE911 CTD profiler mounted on a rosette for all voyages. The profiler was fitted with a Seabird SBE32, 24-Niskin bottle rosette sampler, a biospherical photosynthetically active radiation sensor, a SBE43 oxygen sensor, a Chelsea Aqua tracker Fluorometer, and a Wetlabs C-Star™ transmissometer. Dissolved inorganic nutrients were analyzed with a Lachat Autoanalyser. NO₃⁻/NO₂⁻ and NH₄⁺ concentrations were measured with detection limits to 0.015 μmol L⁻¹ and phosphate and silicate concentrations with detection limits to 0.01 μmol L⁻¹.

For high-performance liquid chromatography (HPLC) analyses, 4-liter samples were filtered on to GF/F filters (nominal porosity of 0.7 μm) from surface and the chlorophyll maximum depth. Analyses were executed with Waters instrumentation (a Waters 996 Photodiode Array Detector, a Waters 600 Controller, and a Waters 717plus Autosampler). The HPLC system used an SGE 250*4.6 mm SS Exsil ODS (octadecyl silica) 5 μm column. Pigments were eluted over a 30-min period with a flow rate of 1 mL min⁻¹. The gradient used follows (Wright et al. 1991): (1) 80:20 (v/v) methanol : ammonium acetate buffer 0.5 mol L⁻¹ pH of 7.2; (2) 90:10 (v/v) acetonitrile : MilliQ water; (3) 100% ethyl acetate. Each solvent was prefiltered through a Millipore HVLP 0.45 μm filter. The separated pigments were detected at 436 nm and identified against standard spectra using Empower™ software. Concentrations of the pigments were determined from standard (Sigma and purified pigments obtained from algal cultures).

To measure PP during the 2003 voyage, gently mixed samples were poured into one dark and two clear 140-mL polycarbonate bottles to which 20 μCi of NaH¹⁴CO₃ were added. Bottles were

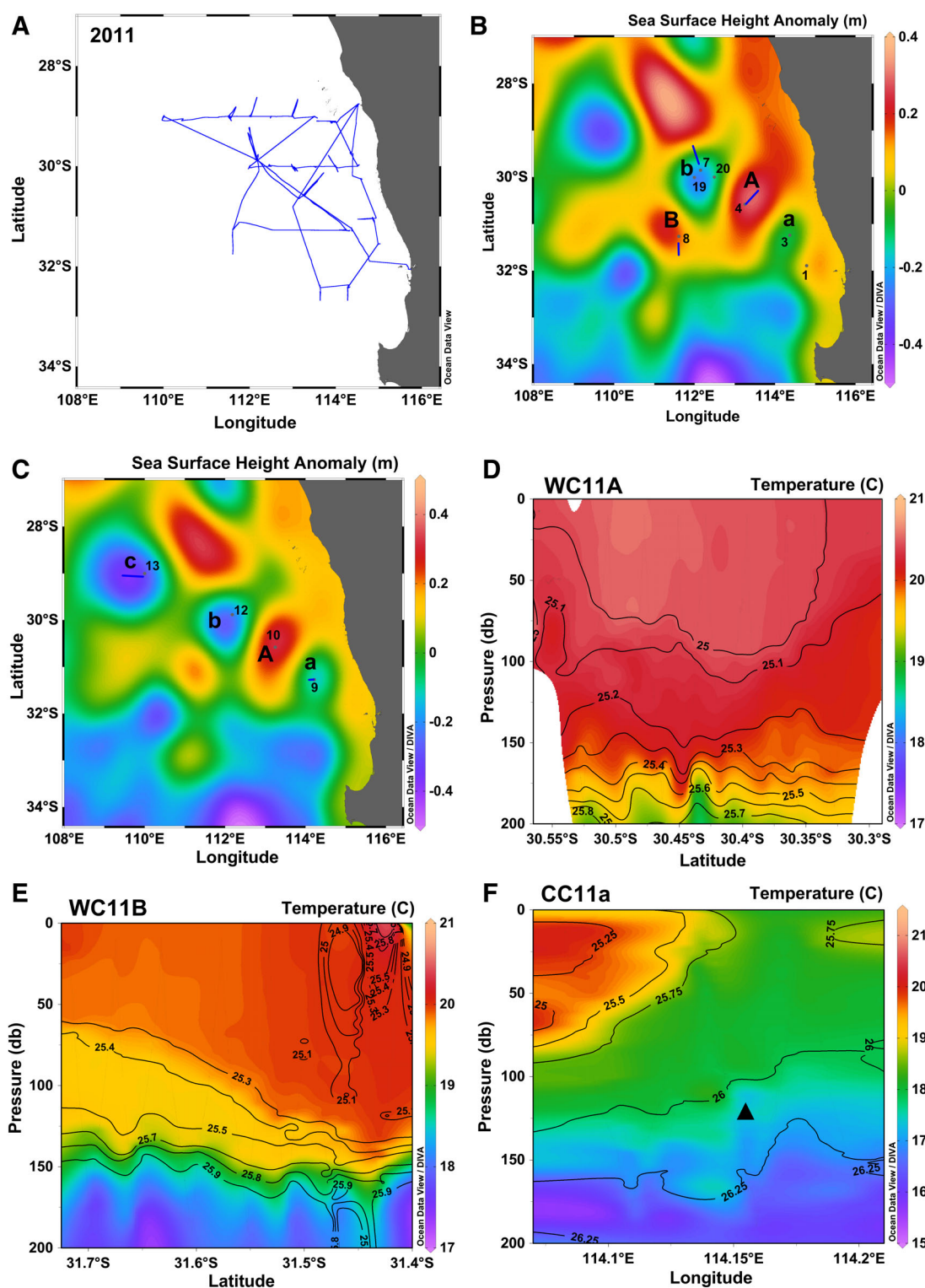


Fig. 3. Ship track and cross-sections of WCEs and CCEs sampled in 2011. (A) Ship track in 2011 showing survey of two WCEs and three CCEs. (B, C) Study region in 2011, showing the large eddy field in the eastern Indian Ocean, with CCEs indicated as negative SSH, and WCEs as positive SSH over two time periods (B: 25–28 August; C: 29 August–01 September). Warm-core (anticyclonic) eddies sampled are labeled with upper case letters (two eddies, WC11A and WC11B) and cold-core (cyclonic) eddies with lower case letters (three eddies, CC11a, CC11b, and CC11c). Other than c, which was sampled once, all eddies were sampled 2–3 times over 2 weeks. (D–H) Towed CTD surveys executed from eddy perimeters to ~centers for the five mesoscale features identified in (B, C) (WC11A, WC11B, CC11a–c, as indicated) with a filled triangle indicating the location of CC11a for clarity.

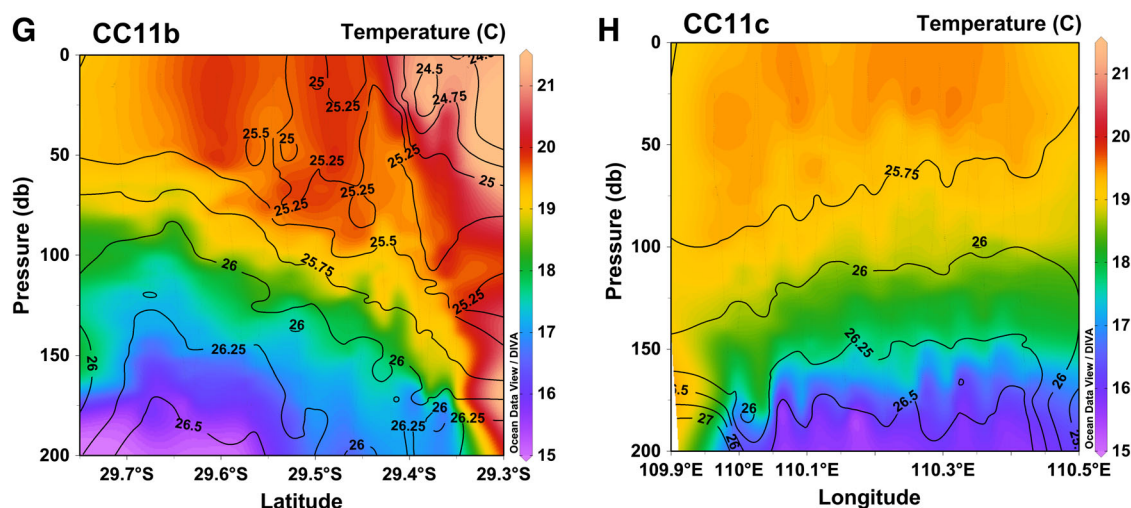


Fig. 3. (Continued).

incubated on deck from dawn-to-dawn (24 h) in Plexiglass tubes covered with a range of blue and neutral films that simulate the intensity and nature of the underwater light field within the euphotic zone. Seawater pumped from 5 m below surface filled the incubator tubes and flowed continuously under pressure to keep samples at near-surface water temperatures. Incubations were terminated in the dark by pouring the content of each incubation bottle through a 25-mm-diameter disk of nylon textile (Nitetex™ mesh size 5 μm) and a Whatman GF/F™ filter placed in series. The filters were dropped into separate borosilicate vials and HCl was added on the filters (250 mL of 0.5 mol L^{-1}) in order to remove nonincorporated ^{14}C . Vials were left open in a fume hood overnight or until the HCl had evaporated and the filters were dry. The activity was measured on a LKB RackBeta™ after adding 10 mL of scintillation cocktail. Carbon uptake was calculated using a value of 26,900 mg C m^{-3} for the concentration of dissolved inorganic carbon.

On the 2006 and 2011 voyages, PP was measured using $\text{NaH}^{13}\text{CO}_3$ rather than $\text{NaH}^{14}\text{CO}_3$. Experiments were initiated by inoculating the water samples with 20 $\mu\text{mol L}^{-1}$ of $\text{NaH}^{13}\text{CO}_3$. Polycarbonate bottles were placed in temperature-regulated on-deck incubators. A range of neutral density screens was used to compensate for the light attenuation at different depths. All polycarbonate incubation bottles were acid-washed, rinsed with deionized water prior to sampling and rinsed three times with seawater directly from sample point prior to incubation. The inoculated water samples were incubated for 6 h (from 08:00 to 14:00 h) and the values scaled to 24 h using local day length.

Five hundred milliliter samples for light microscopy were preserved in Lugol's solution (Parsons et al. 1984) and examined following protocols given in Hötzel and Croome (1999). An Olympus BX 51 microscope and a magnification of 400X were used to enumerate and classify cells. Cells were classified at the class level and, where identifiable at 400X magnification, the top 10 taxa were identified to genus or to species level.

Rock lobster larvae were collected to 200 m depth using a multiple opening and closing EZ net with a 1 m^2 opening. In 2010 and 2011, additional tows were conducted at night using 10-min surface tows with a 1 m^2 opening net. The latter procedure increased sampling success and allowed us to increase our sample size. Zooplankton were collected via oblique bongo net hauls from 150 m, sorted immediately by size (through a screen stack of 4000, 2000, 1000, 500, 300, and 100 μm) and by organism type (chaetognaths, salps, copepods, and euphausiids), and snap-frozen in cryovials at -80°C for later analysis. Particulate organic matter was sampled as 4 L of seawater filtered gently on to precombusted 25 mm GF/F filters, then also snap-frozen for later analysis.

In 2003, 2010, and 2011, determination of total C, total N, $\delta^{13}\text{C}$, and $\delta^{15}\text{N}$ on the size-fractionated and species-sorted net samples, as well as the particulate organic matter samples were undertaken using a continuous flow system consisting of a SERCON 20–22 mass spectrometer connected with an automated nitrogen carbon analyzer. Multipoint normalization was used in order to reduce raw values to the international scale (Paul et al. 2007). Error propagation for stable isotope data was performed as described by Skrzypek et al. (2010). The external error of analyses (1 standard deviation) was 0.15‰ for $\delta^{13}\text{C}$ and 0.20‰ for $\delta^{15}\text{N}$. In 2006, all stable isotope measurements were made by continuous-flow isotope-ratio mass spectrometry using a Micro-mass Optima interfaced to a CE NC2500 elemental analyzer (at the Georgia Institute of Technology) for online combustion and purification of sample nitrogen and carbon. All stable isotope abundances are reported as $\delta^{15}\text{N}$ and $\delta^{13}\text{C}$ values relative to atmospheric N_2 and Vienna Pee Dee Belemnite standard, respectively. Each analytical run included a size series of elemental (acetanilide or methionine) and isotopic (peptone) standards, which provided a check on the stability of the instrument and allowed us to remove the contribution of any analytical blank from our isotopic measurements (Montoya 2008). We conservatively estimate that

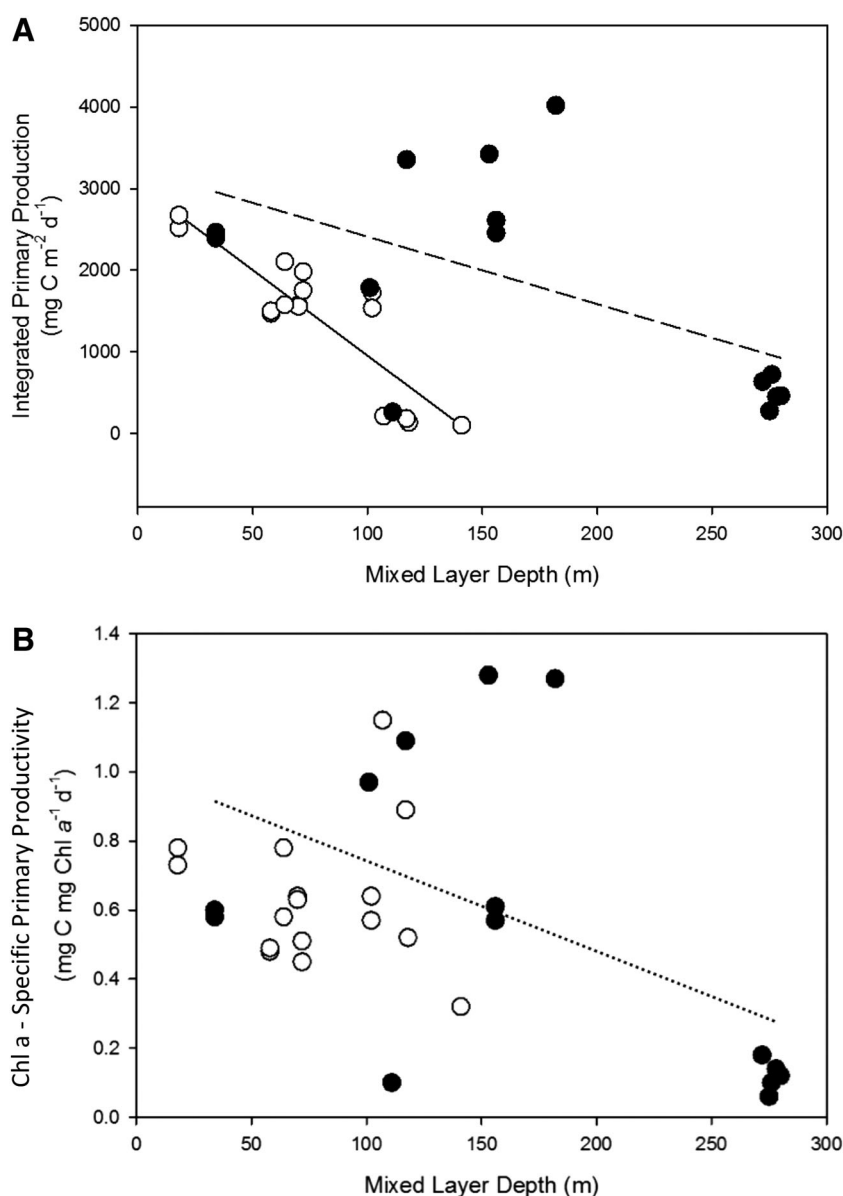


Fig. 4. Depth-integrated PP and Chl *a*-specific productivity plotted against MLD across eight eddies. Each point represents one CTD cast/oceanographic station. **(A)** Total C-fixation per unit area ($\text{mg C m}^{-2} \text{d}^{-1}$), with significant line of best fit (CCEs solid line, $p < 0.001$; WCEs dashed line $p < 0.05$). **(B)** Chlorophyll-specific productivity ($\text{mg C / mg Chl } a \text{ d}^{-1}$). The dashed line indicates lines of best fit for WCEs ($p < 0.05$), not significant for CCEs.

the overall analytical precision of our isotopic measurements is better than 0.1% (Montoya 2008).

The effect of eddy (WCE vs. CCE) and year (2003 vs. 2011, not available for the 2006 eddy) on phytoplankton composition (%diatom and %dinoflagellates in cell counts) were compared using a two-way ANOVA against eddy and year. A two-way ANOVA was used to test the effect of eddy (WCE vs. CCE) and filtered size fraction (> 5 vs. $< 5 \mu\text{m}$) on three key phytoplankton pigment fractions (divinyl Chl *a*, diadinoxanthin, and fucoxanthin; see Waite et al. 2007b) normalized to total Chl *a*.

MLDs were calculated according to de Boyer Montégut et al. (2004) as a ΔT decrease of 0.4°C compared to a reference value

at 6 m depth. Statistical analyses were performed in the R statistical package v3.0.1 (R Core Team 2013). The effect of mixed-layer depth on integrated PP and Chl *a*-specific productivity, were tested using linear regression (Sigmaplot14[®]) for WCEs and for CCEs, respectively.

Because data were non-normal, a Mann–Whitney rank sum test was used to test the effect of eddy type on $\delta^{15}\text{N}$ and $\delta^{13}\text{C}$ of size-fractionated zooplankton across all eddies. The effects of organism size and MLD on size-fractionated zooplankton $\delta^{15}\text{N}$ and $\delta^{13}\text{C}$ were then tested across all eddies sampled in all years (2003, 2006, 2011) using a two-way ANOVA conducted using the car-package (Fox and Weisberg 2010) for R with a

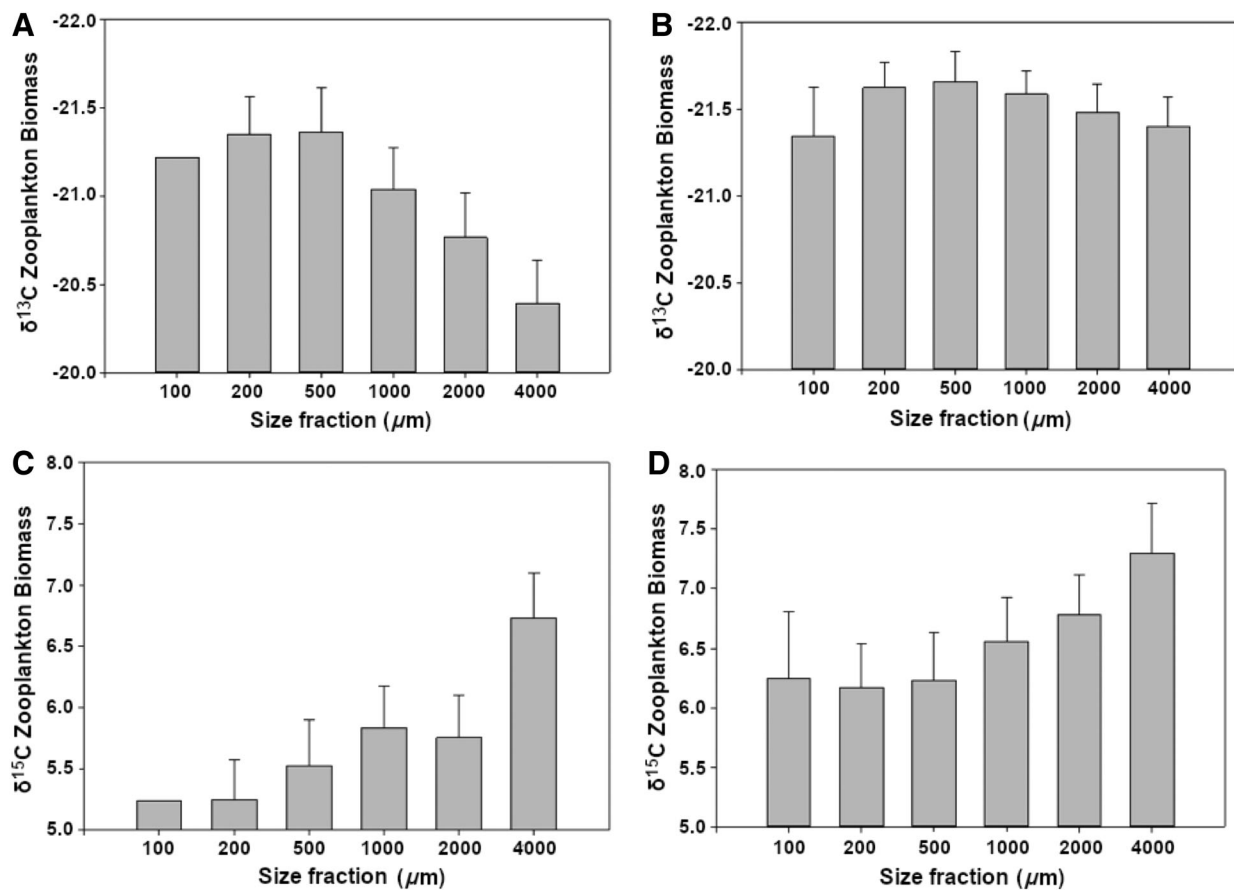


Fig. 5. Mean isotopic signatures ($\delta^{15}\text{N}$ and $\delta^{13}\text{C}$) of size-fractionated bulk zooplankton samples (sieved through 100, 200, 500, 1000, 2000, and 4000 μm meshes) across all eddies in all years (2003, 2006, 2011), with the effect of MLD removed (via two-way ANOVA; for MLD effects, see Fig. 6A,B). (A) $\delta^{13}\text{C}$ of zooplankton from WCEs. (B) $\delta^{13}\text{C}$ of zooplankton from CCEs. (C) $\delta^{15}\text{N}$ of zooplankton from WCEs. (D) $\delta^{15}\text{N}$ of zooplankton from CCEs. Error bars represent standard error of the means.

linear regression model, based on a heteroscedasticity consistent covariance matrix, as sample size was < 250 (Long and Ervin 2000). Statistical relationships between isotopic zooplankton composition and MLD were quantified through linear and nonlinear regression using Sigmaplot14[®]. Interannual differences in rock lobster phyllosoma $\delta^{15}\text{N}$ and $\delta^{13}\text{C}$ signatures were tested using one-way ANOVA between 2010 and 2011. Differences in size fractionated zooplankton $\delta^{15}\text{N}$ and $\delta^{13}\text{C}$ signatures between 2010 and 2011 were tested using a two-way ANOVA on size and year, followed by size-specific and year-specific comparisons using the Holm-Sidak method (Sigmaplot14[®]). The $\delta^{15}\text{N}$ and $\delta^{13}\text{C}$ signatures of individual zooplankton groups (krill, copepods, chaetognaths, and salps) were also compared between 2010 and 2011 using a one-way ANOVA.

Results

We present data from eight mesoscale eddies formed offshore of the LC system in the eastern Indian Ocean off Western Australia (four WCEs and four CCEs). These include one WCE and one CCE in 2003 for which many data are already

published (Fig. 1A–F) (Waite et al. 2007a), one WC eddy studied in 2006 (Fig. 2A–C) (Paterson et al. 2008; Waite et al. 2016a,b) and five eddies (two WC and three CC) studied in 2011 associated with rock lobster larval sampling (Table 1; Fig. 3A–H). SSHA plots for each eddy highlight the CCEs (negative SSHA = CC) and WCEs (positive SSHA = WC), as well as the sampling locations in each eddy. For the 2003 eddies, and for the single WC eddy sampled in 2006, we present up to six CTD profiles per eddy, as eddies were sampled repeatedly over 3 weeks (CC03 and WC03, and WC06). In 2011, each of the five eddies (CC-a,b,c, and WC-A,B) was sampled sequentially up to three times. However, the 2011 eddies were not surveyed in detail as with the 2003 and 2006 studies. From 2010, we present the results of a regional survey not targeting eddies specifically (Fig. 2D,E).

The MLD of CCEs was about half that of the WCEs (Table 1), and both depth-integrated Chl *a* (to 150 m) and PP rates in CCEs were about 40% lower than WCEs (Table 1). A two-way ANOVA comparing the cell count data between eddies (WCE vs. CCE) and across years (2003 vs. 2011, not available for the 2006 eddy) indicated that across both years, WCEs had overall higher

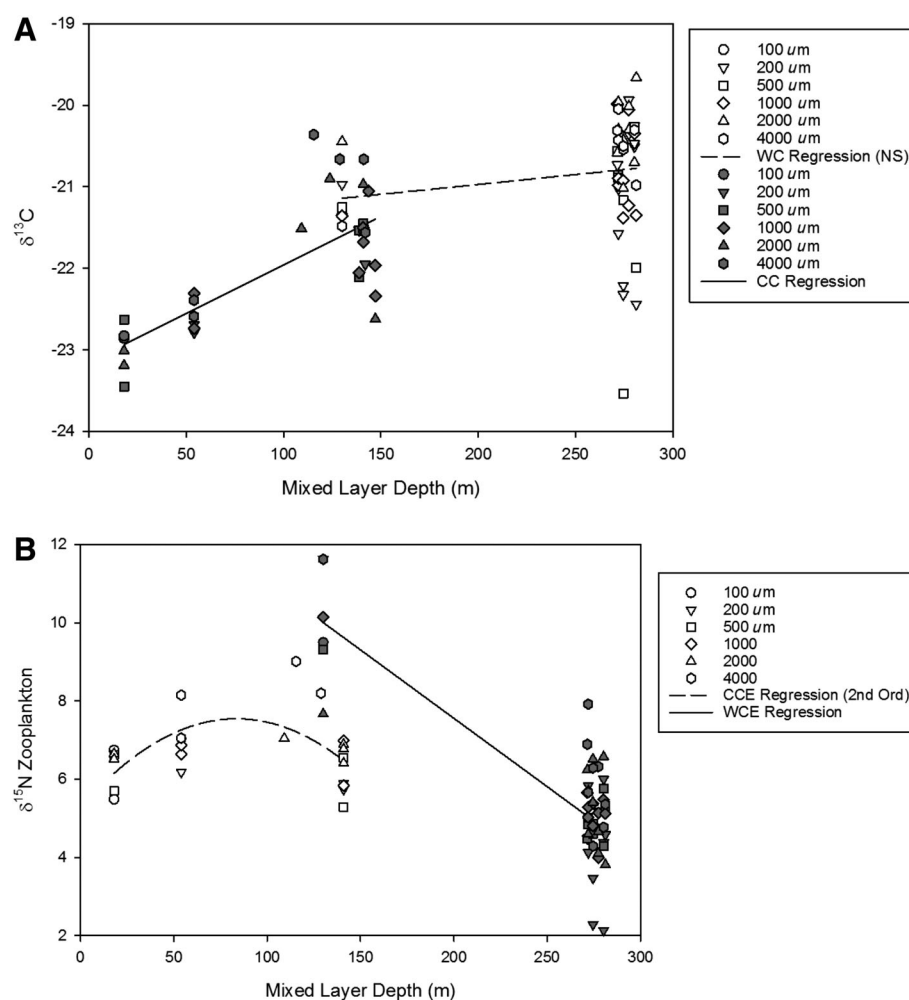


Fig. 6. Zooplankton $\delta^{15}\text{N}$ and $\delta^{13}\text{C}$ as a function of MLD for eight eddies in the study region between 2003 and 2011, plotted as individual size categories for each station, showing relationships between CCEs and WCEs. **(A)** Size-fractionated zooplankton $\delta^{13}\text{C}$ data, with WCEs shown in black symbols, CC data in open symbols. The solid line indicates the relationship between MLD and $\delta^{13}\text{C}$ in CCEs; the dashed line is the nonsignificant line for WCEs. For CCEs, there is a strong indication ($r^2 = 0.46$) for lighter $\delta^{13}\text{C}$ zooplankton at shallower MLD. **(B)** Size-fractionated zooplankton $\delta^{15}\text{N}$ data with WCEs shown in gray symbols, CC data in open symbols. The solid lines indicate significant relationships between MLD and $\delta^{15}\text{N}$ in WC (linear relationship) and CC (hyperbolic relationship) eddies.

%diatoms ($p < 0.001$) and that the 2003 eddies were higher in %diatoms than in those sampled in 2011 ($p < 0.011$). Pigment analyses indicated no overall difference between WCEs and CCEs in the diadinoxanthin–Chl *a* ratio, but fucoxanthin/Chl *a* in WCEs was about four times that in CCEs ($p < 0.001$), particularly in the large ($> 5 \mu\text{m}$) size fraction, since the fucoxanthin fraction was almost undetectable in CCEs. divinyl-Chl *a*/Chl *a* was about four times higher in CC than in WCEs. Overall, this indicates significantly higher diatom fractions in WCEs, and a greater predominance of picoplankton in CCEs. Dinoflagellate abundance, including heterotrophs, represented over 50% of all cell counts in both eddy types (Table 1).

Relationships between integrated PP and MLD showed different relationships with MLD for WCEs and CCEs (Fig. 4A). Integrated primary productivity was greater in CCEs with shallower MLDs ($\text{df} = 14$; $p < 0.001$). This was also true in WCEs but the relationship was weaker ($\text{df} = 13$; $p < 0.05$) (Fig. 4A). The

Chl *a*-specific productivity of both WCEs and CCEs were similar (across all eddies and both years specific production was $\sim 0.67 \pm 0.22 \text{ mmol C mg Chl } a^{-1} \text{ d}^{-1}$). There was a weak tendency ($p = 0.05$) for WCE Chl *a*-specific productivity to decrease with increasing MLD, but no relationship for CCEs (Fig. 4B).

Two-way ANOVA across all size-fractionated zooplankton $\delta^{13}\text{C}$ values in all eddies vs. organism size fraction and MLD showed significant differences in WCEs ($p = 0.002$; Fig. 5A), but no differences across zooplankton size fractions in CCEs ($p = 0.74$; Fig. 5B). $\delta^{13}\text{C}$ varied with MLD in both eddy types (both $p < 0.001$), see also Fig. 6A. Two-way ANOVA across all size-fractionated zooplankton $\delta^{15}\text{N}$ data in all eddies vs. organism size and MLD indicated a marginal increase in $\delta^{15}\text{N}$ with increasing size fraction for WCEs (Fig. 5C; $p = 0.058$) but no significant differences in $\delta^{15}\text{N}$ across organism size fraction ($p = 0.30$) in CCEs (Fig. 5D). $\delta^{15}\text{N}$ varied statistically with MLD within both CC and WCEs (two-way ANOVA $p = 0.016$ and $p = 0.001$ for

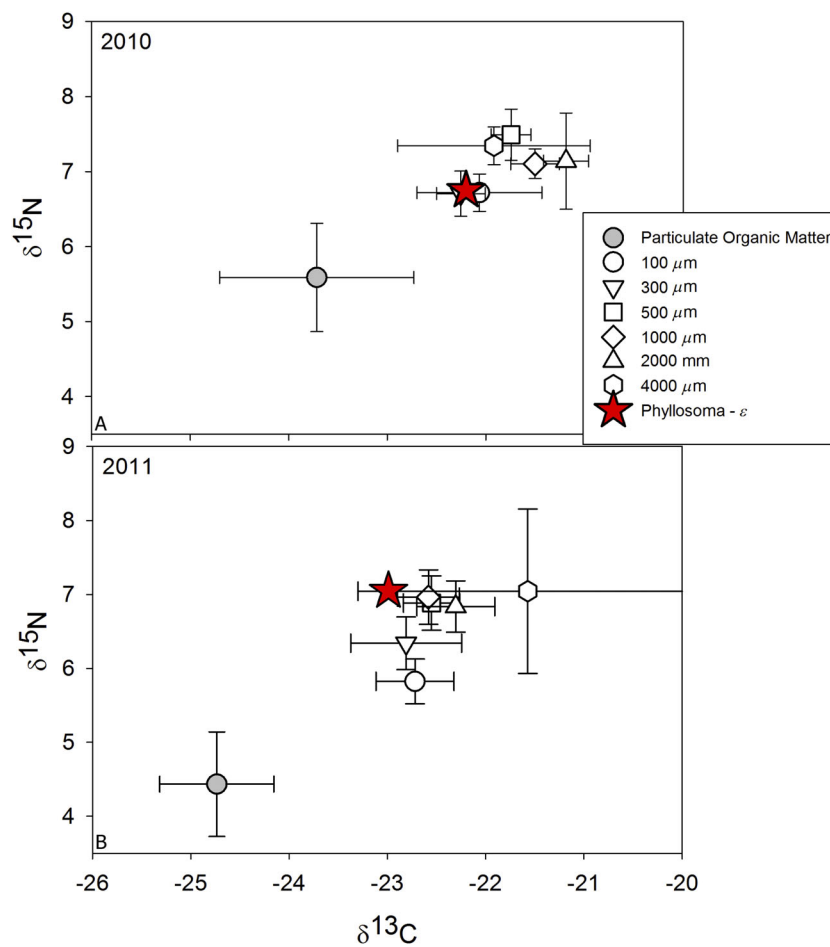


Fig. 7. Comparison of rock lobster phyllosoma and the bulk size-fractionated zooplankton isoscape and particulate organic matter. Mean isotopic signatures ($\delta^{15}\text{N}$ and $\delta^{13}\text{C}$) of western rock lobster phyllosoma larvae (minus enrichment factor ϵ from Waite et al. 2007a; $\epsilon = 1.7 \delta^{15}\text{N}$ and $1 \delta^{13}\text{C}$ unit) shown as red stars (for raw data, see Fig. 8A), with size-fractionated zooplankton $\delta^{15}\text{N}$ and $\delta^{13}\text{C}$ (open symbols) and particulate organic matter (gray symbol), over 2 yr: (A) 2010 and (B) 2011.

CC and WC, respectively). Overall, zooplankton in WCEs had significantly lower $\delta^{15}\text{N}$ (median CC = 6.63 vs. WC = 5.19, Mann–Whitney rank sum test $p < 0.001$) and significantly heavier (less negative) $\delta^{13}\text{C}$ (median CC = -21.995 vs. WC = -20.582 , Mann–Whitney rank sum test $p < 0.001$).

There were significant statistical relationships between size-fractionated zooplankton isotopic signature and MLD (Fig. 6A,B). The relationships for $\delta^{15}\text{N}$ and $\delta^{13}\text{C}$ were qualitatively different; $\delta^{13}\text{C}$ signature became more negative with increasing MLD for CCEs (Fig. 6A, $r^2 = 0.46$, $a = 0.015\text{‰} \delta^{13}\text{C} \text{ m}^{-1}$, $p < 0.001$), while the $\delta^{15}\text{N}$ values across all zooplankton size fractions showed an inverse hyperbolic relationship with MLD for CCEs (Fig. 6B), and an apparent decrease with MLD for WCEs (with only $n = 2$ eddies here, this significance is probably marginal for interpretation).

The significant differences in the zooplankton isotopic signatures between WC and CCEs across all years (above) were then compared with the interannual variation in size-fractionated zooplankton isotopic signatures (2010 vs. 2011; Fig. 7A,B) from broader sampling across the study region, including all eddy and

noneddy samples 2010–2011 (for ship tracks and station locations, see Figs. 2D,E, 3A–C). There were regionally consistent differences between the 2 yr, with zooplankton in 2011 (a strong La Niña year) statistically $0.64 \delta^{13}\text{C}$ units lighter (more negative), and $0.43 \delta^{15}\text{N}$ higher, than in 2010 (an El Niño year). Across all years, size was a significant factor structuring $\delta^{15}\text{N}$, but not $\delta^{13}\text{C}$ (two-way ANOVA vs. year and size fraction: for $\delta^{13}\text{C}$, Year $p < 0.001$, Size $p = 0.067$; for $\delta^{15}\text{N}$, Year $p < 0.001$, Size $p < 0.001$). Note that this regional interannual difference is about half of the difference between WC and CCEs ($\Delta 1.41 \delta^{13}\text{C}$ units, and $\Delta 1.44 \delta^{15}\text{N}$ units, see above).

The mean isotopic signatures ($\delta^{15}\text{N}$ and $\delta^{13}\text{C}$) of western rock lobster phyllosoma in 2010 and 2011 across the study region (eddy and non-eddy included) were then compared with those of their potential prey, the bulk size-fractionated zooplankton, using the regional N-isotopic enrichment factor (1.7 per trophic level) calculated by Waite et al. (2007a) (Fig. 7A,B). For the 2010 data, phyllosoma $\delta^{15}\text{N}$ and $\delta^{13}\text{C}$ signatures (minus this enrichment factor) overlapped with size-fractionated

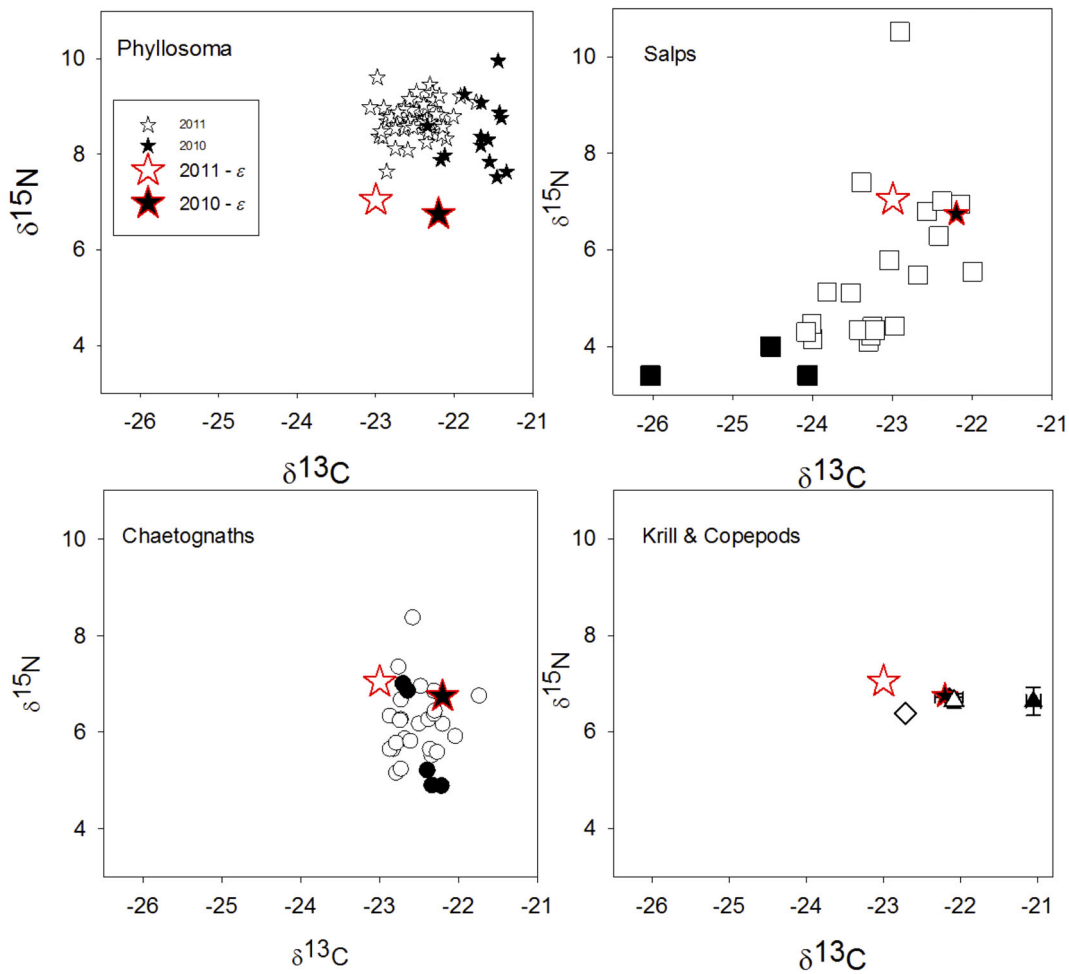


Fig. 8. Comparison of isotope signatures of western rock lobster phyllosoma and their taxonomically selected potential prey across 2010 (black symbols) and 2011 (white symbols). **(A)** Raw isotopic signatures ($\delta^{15}\text{N}$ and $\delta^{13}\text{C}$) of western rock lobster phyllosoma larvae and corrected mean phyllosoma isotope signature (minus the enrichment factor ϵ from Waite et al. 2007a; $\epsilon = 1.7 \delta^{15}\text{N}$ and $1 \delta^{13}\text{C}$ unit). **(B)** Salp isotopic signatures ($\delta^{15}\text{N}$ and $\delta^{13}\text{C}$) with corrected phyllosoma signatures (symbols as in **A**). **(C)** Chaetognath isotopic signatures ($\delta^{15}\text{N}$ and $\delta^{13}\text{C}$) and corrected phyllosoma signatures (symbols as in **A**). **(D)** Copepod and krill isotopic signatures ($\delta^{15}\text{N}$ and $\delta^{13}\text{C}$) as means and standard errors where error bars are not visible they are smaller than symbol size. Corrected phyllosoma signatures have symbols as in Fig. 6A.

zooplankton signatures from the 100–300 μm fraction zooplankton in 2010 (Fig. 7A). A larger data set in 2011 showed the phyllosoma overlapping in isotopic signature with zooplankton of a possibly larger mean size (1000–4000 μm fraction). Isotopic signatures of phyllosomas were not highly variable regionally across four degrees of latitude (coefficient of variation [CV] = 8% for $\delta^{15}\text{N}$, and 1% for $\delta^{13}\text{C}$ within each year).

In taxonomically separated samples (Fig. 8A–D), phyllosomas' most abundant potential zooplankton prey, the krill and copepods, showed a statistical decrease regionally between 2010 and 2011 as the bulk zooplankton samples, on the order of 1‰ $\delta^{13}\text{C}$ (Table 2; Fig. 8A,C,D), suggesting a regionally consistent, interannually varying isoscape. Salp isotopic signatures, in contrast, were much more variable, particularly in $\delta^{15}\text{N}$, and did not show a clear covariation between years (Fig. 8B). Across all years, salps were present primarily in the larger size fractions (4000 μm). The large data scatter of the isotopic $\delta^{15}\text{N}$ signature

of salps (between 3–11‰) increased the total variation in the 4000 μm size fraction.

A paucity of samples still limits the statistical resolution of possible linkages between isotopic signatures of phyllosoma and their key prey (Table 2), and significantly more data are needed to resolve any long-term connection between prey and predator.

Discussion

We posed the question as to why, in our recent work, rock lobster phyllosoma in CCEs are significantly healthier, with larger lipid stores, than those in WCEs (Wang et al. 2014a, 2015). We hypothesized that CCEs were more productive than WCEs, but we disprove this hypothesis. We conclude that despite CCEs and WCEs hosting similar Chl *a*-specific productivity, CCEs support a nutritionally advantageous ecosystem

Table 2. Comparison of mean $\delta^{13}\text{C}$ signatures of phyllosoma and possible zooplankton prey groups, for 2003 data already published (Waite et al. 2007a), a small number of samples in 2006, and for the 2010 and 2011 measurements which are presented for the first time in this study, and shown in Fig. 8A–D.

Mean $\delta^{13}\text{C}$ for zooplankton groups	2003 ⁺ (SE) <i>n</i>	2006 (SE) <i>n</i>	2010 (SE) <i>n</i>	2011 (SE) <i>n</i>	Significant difference (2010 vs. 2011)
Phyllosomas	−21.9* (0.71) 2	−20.78 ^x <i>n</i> = 1	−21.7 (0.08) 15	−22.3* (0.07) 24 −21.6 ^x (0.11) 14	<i>p</i> < 0.001
Chaetognaths	−19.73 ^x (0.48) 2	−20.01 ^x (0.22) 23	−22.5 (0.09) 5	−22.6 (0.02) 22	NS
Salps	−21.8 ^x (0.90) 4	−23.96 ^x (1.8) 4	−24.9 (0.51) 4	−23.31 (0.14) 16	<i>p</i> < 0.001
Copepods	−21.2 ^x (0.12) 4 −23.4* <i>n</i> = 1	−21.18 ^x (0.15) 27	−22.1 (0.22) 6	−22.7 (0.06) 47	<i>p</i> < 0.05
Krill	−20.1 (0.56) 3	−19.96 ^x (0.36) 32	−21.0 (0.11) 4	−22.1 (0.06) 21	<i>p</i> < 0.0001

Larger sample sizes from targeted rock lobster larval sampling in 2010 and 2011 (also shown in Fig. 8A–D) allowed a statistical comparison between the 2 yr. Values shown are means, (standard error), and sample size *n*. Where available, * designates CCE samples and ^x indicates WCE samples. + indicates data already published in Waite et al. (2007a).

for zooplankton, based on flagellate/dinoflagellate productivity that favors improved zooplankton lipid stores and ultimately phyllosoma health. In contrast, WCE ecosystems, with higher prevalence of diatoms, are less favorable for phyllosomas. For both eddy types, depth-integrated productivity was higher in eddies with shallower mixed layers (MLs), but this was especially pronounced in CCEs (where PP is concentrated below, rather than throughout, the ML). MLs tend to be shallower in CCEs than WCEs overall because the pycnocline is closer to the surface in CCEs, inhibiting wind-driven overturning. Stronger stratification in the CCE pycnocline (Greenwood et al. 2007) would favor flagellates over diatoms (Cushing 1989).

The south-eastern Indian Ocean off Australia is highly oligotrophic and temperature-stratified, such that surface waters are often completely depleted of nutrients, particularly nitrogen. At the shelf-break, the southward-flowing LC follows the ~ 200 m shelf-edge contour (Hanson et al. 2007). Nutrients are delivered sporadically throughout the year by topographically controlled upwelling (Rossi et al. 2013) and by vertical mixing in the deepening ML of the LC in the autumn (Rousseaux et al. 2012). Water column productivity is thus dominated for most of the year by the productivity of the DCM, which is embedded in the pycnocline/nutricline. Productivity of the DCM is tightly controlled by the MLD, with shallower DCMs showing higher productivity, and deeper DCMs having lower productivity across the region (Hanson et al. 2007; Feng et al. 2009).

Within this system, CCEs represent locally intensified stratification, with the pycnocline lifted physically into the euphotic zone, accelerating production near the eddy center (see Waite et al. 2007a,b) while largely hidden from remote sensing (“cryptic”; sensu Hanson et al. 2007). WCEs, on the other hand, have their biomass mixed through a deep surface ML whose productivity slowly declines with time after nutrient injection (Greenwood et al. 2007). Nutrient injection into WCEs occurs near the coast during eddy formation (Waite et al. 2016 a,b) and/or during winter mixing (Dufois et al. 2016).

We show here that Chl *a*-specific productivity in CCEs and WCEs is about equal. Shallowing of MLDs through CCE formation is likely a key bottom-up mechanism driving production in CCEs, but we find that this alone is not enough to account for healthier phyllosomas in CCEs. As elucidated below, our isotope data suggest that CCEs may host zooplankton with superior lipid stores (inferred from $\delta^{13}\text{C}$) operating at a lower trophic level (inferred from $\delta^{15}\text{N}$) making them significantly better nutritional value to the phyllosomas.

The $\delta^{13}\text{C}$ of zooplankton is strongly impacted by the lipid content of the organisms themselves: Lipids have an extremely negative $\delta^{13}\text{C}$ signature (light to very light at −24 to −36, (Morris et al. 1971). Heavy $\delta^{13}\text{C}$ s have thus been proposed as an index of nutritional stress (McCue 2012). Zooplankton stripped of their lipid load have isotope signatures on average around 1.4‰ $\delta^{13}\text{C}$ heavier than zooplankton with their lipid stores intact (Sato et al. 2002), while amino acids have a much heavier $\delta^{13}\text{C}$ signature (= −15‰ to −20‰; Hannides et al. 2013) and thus would bring starved zooplankton signatures toward heavier, less negative, values.

The median zooplankton $\delta^{13}\text{C}$, a putative index of the organism’s lipid content (Sato et al. 2002), was higher in CCEs than in WCEs overall, suggesting that zooplankton living in CCEs may have higher lipid stores, consistent with comparative measures in phyllosomas (Wang et al. 2014a). The size-specific comparison between WCE and CCEs showed that the $\delta^{13}\text{C}$ zooplankton in WCEs declined with organism size (Fig. 5); one interpretation of this is that the lipid fraction declined with trophic level. In CCEs, the $\delta^{13}\text{C}$ signature showed no statistical change with size, which might suggest that the lipid content was stable with trophic level, such that organisms at higher trophic levels were overall richer in lipid. The correlation between $\delta^{13}\text{C}$ values and MLD (Fig. 6A) is thus likely to reflect the higher lipid stores of zooplankton incubated in CCEs vs. WCEs.

The CCEs and WCEs also showed significantly different size-specific zooplankton $\delta^{15}\text{N}$ signatures, supporting the notion that

the zooplankton community is differently structured. In earlier work, we showed that nitrogen isotopic signatures of zooplankton in this region (hereafter the “isoscape”) are primarily driven (1) by increases in MLD (+1.5 $\delta^{15}\text{N}$ units per 100 m), and (2) trophic level (\sim organism size: +1.7 $\delta^{15}\text{N}$ per trophic level) (Waite et al. 2007a, b). The difference in zooplankton $\delta^{15}\text{N}$ between the two eddy types in this study (\sim 1.4 $\delta^{15}\text{N}$ units) could therefore be explained simply by the difference in mean MLD (\sim 153 m [WCEs] vs. \sim 85 m [CCEs]) between the two eddy types. This would be consistent with the occurrence of higher nitrate fluxes into the euphotic zone of eddies with shallower MLDs, regionally increasing production rates as the MLD shallows.

The relationship between zooplankton $\delta^{15}\text{N}$ and MLD, however, shows something more complex for CCEs—a reduction of $\delta^{15}\text{N}$ by just over 1 $\delta^{15}\text{N}$ unit at the shallowest MLD, such that the relationship between $\delta^{15}\text{N}$ and MLD is statistically more hyperbolic than linear ($\text{df} = 23$, $p < 0.01$ for a second order curve, see Fig. 6B). It could be inferred from this that zooplankton in CCEs with the shallowest MLD are feeding at about 0.6 of a trophic level lower than expected. In eddies with MLDs of about 150 m (Fig. 6B), WCE zooplankton $\delta^{15}\text{N}$ signatures are about 2.5 $\delta^{15}\text{N}$ units higher than their CCE counterparts, suggesting the zooplankton at the same size categories are operating about 1.5 trophic levels higher in WCEs than in CCEs. Together, these data support the notion

that CCEs with the shallowest MLDs have efficient trophic transfer and a lower mean trophic level than WCEs.

This is interesting given the predominance of dinoflagellate and cryptophyte biomass in CCEs (Thompson et al. 2007; this article). One mechanism by which healthy phyllosomas might be supported in CCEs is through altered ecosystem structure supporting highly coupled grazing rates and more effective trophic transfer, lowering biomass in CCEs. The higher concentration of diatoms in WCEs could provide one explanation for their less healthy larvae. Diatoms are known as having a strong resistance to copepod grazing (Friedrichs et al. 2013), to the point of strongly influencing ecosystem structure and associated vertical Si and C fluxes (Assmy et al. 2013). A diatom-dominated ecosystem in a WCE might therefore be harder to graze.

In addition, while small dinoflagellates and diatoms growing under optimal conditions are similar in lipid content (Finkel et al. 2016a,b), large dinoflagellates ($> 320 \mu\text{m}^3$) are statistically about two times richer in energy per cell, increasing still further in larger cells (Finkel et al. 2016a), and under nutrient deplete conditions (Mansour et al. 2003). Under these conditions, dinoflagellates can provide better nutritional value to zooplankton than diatoms (Hitchcock 1982; Jones and Flynn 2005), including the provision of long-chain fatty acids, such as docosahexaenoic acid, which are critical for larval condition (Stoecker and Capuzzo 1990).

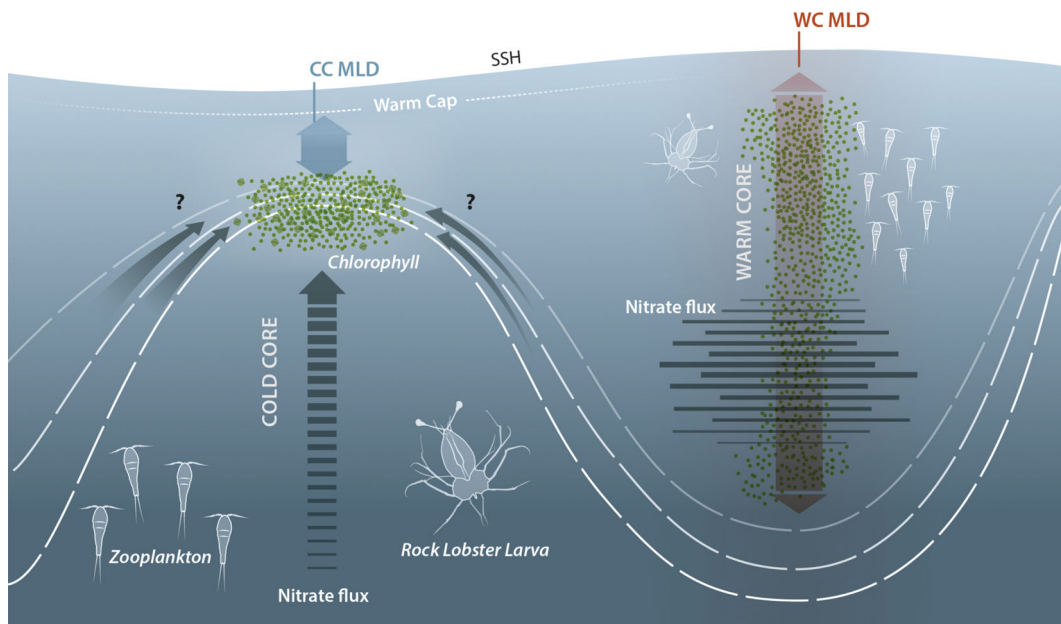


Fig. 9. Conceptual model. A conceptual model for the bottom-up physical control of phyllosoma larval health by WCEs and CCEs, respectively. For both eddy types, the PP/Chl *a* is constant. Integrated PP is negatively correlated with MLD in both eddy types (see Fig. 4A) but is more tightly controlled by depth of the chlorophyll maximum/pycnocline in the highly stratified CCEs. In CCEs, upwelled and/or along-isopycnal nitrate supply is maintained, but precise flux mechanisms are still unclear (hence “?” annotation) (Feng et al. 2007; Pidcock et al. 2016). In WCEs, nitrate supply decreases with time after initial (or seasonal) nutrient injection (Greenwood et al. 2007; Dufois et al. 2016) more analogous to a batch culture. In CCEs, flagellate and dinoflagellate populations provide easily grazed high-quality nutrition for zooplankton, which feed on average at a low trophic level and maintain high lipid stores. CCEs thus function in a manner analogous to a chemostat culture. In contrast, WCEs have, on average, deeper MLs, and a phytoplankton community with more diatom predominance. Diatoms provide a lower quality food for zooplankton, and thus zooplankton lipid stores in WCEs decline with trophic level, and with time after initial (or seasonal) nutrient injection. As a result, phyllosomas have higher energy and lipid content (Wang et al. 2015) in CCEs than in WCEs.

Specific fatty acids and relatively high levels of sterols derived from dinoflagellates have previously been found to provide the dominant food chain signal in the phyllosoma of *P. cygnus* (Phillips et al. 2006). Furthermore, a higher level of fatty acid markers for flagellates and a lower level of copepod grazing markers were found in *P. cygnus* phyllosoma sampled from CCEs vs. WCEs (Wang et al. 2014b).

To explore the MLD-zooplankton relationship to phyllosoma growth, we identified the most likely prey of phyllosomas by comparing $\delta^{13}\text{C}$ and $\delta^{15}\text{N}$ of phyllosomas to most available prey items (only for 2010–2011). When corrected with an enrichment factor of 1.7 $\delta^{15}\text{N}$ and 1 $\delta^{13}\text{C}$ per trophic level (Waite et al. 2007a), the isotope signatures of the phyllosoma overlapped with salps, copepods, chaetognaths, and euphausiids, consistent with a varied zooplankton diet, with chaetognaths and copepods among the most important prey items. However, our earlier work, including gut contents analyses and ship-board experiments, suggests that other organisms can also be a part of the phyllosoma diet (O'Rourke et al. 2012, 2013; Saunders et al. 2012). While a detailed examination of specific isotopic linkages is beyond the scope of this article, we note that the phyllosoma isotopic C signatures did covary interannually (across 2010 and 2011) with that of the zooplankton prey field. This suggests that zooplankton isotopic $\delta^{13}\text{C}$ values, and phyllosoma chemical signatures, may have a regional-scale (i.e., physical oceanographic) source of variation. This could be mechanistically driven via changes in CCE vs. WCE generation, and interannual variation in their mean MLD. However, the most important variations in the pycnocline depth are on the scale of ENSO cycles—on average, the depth is 10 m shallower than average during an El Niño year, and 12 m deeper than average during a La Niña year (Feng et al. 2003). It is possible that regional interannual differences in the zooplankton isoscape we noticed could be linked with these time scales of changes, where the pycnocline changes by 20 m. It is clear from Figs. 4A,B, 6A,B, that a 20 m variation in MLD could have a significant impact both on productivity and on zooplankton chemical composition.

In summary (Fig. 9), PP in CCEs increases where the chlorophyll maximum, embedded in the pycnocline, is closer to the surface, and along-isopycnal nitrate supply can be maintained (Feng et al. 2007; Pidcock et al. 2016). This allows the system to function in a manner analogous to a chemostat culture. Zooplankton in CCEs have significantly higher lipid stores, and CCEs with the shallowest MLDs are the healthiest eddy systems for phyllosoma. In contrast, in WCEs, zooplankton lipid stores decline with time after initial, or seasonal, nutrient injection (Greenwood et al. 2007; Dufois et al. 2016), more analogous to the dynamics of a batch culture.

This conceptual model works best if grazing rates, particularly herbivory, are overall higher in the CCEs, explaining higher zooplankton nutritional status in comparison to the WCEs. Is there evidence for this? Only very indirectly: Waite et al. (2007a) showed that the particulate nitrogen : Chl *a* ratio, known as an indicator of grazing rate (Waser et al. 2000), was about five

times higher in a CCE vs. a WCE. Strzelecki et al. (2007) showed that the same CCE had a much higher abundance and volume of siphonophores which, like other gelatinous zooplankton, are known for their ability to efficiently prey on dispersed plankton resources over a wide range of sizes and potentially improving trophic transfer of PP (Mills 1995; Purcell 1997), while also providing a food source for phyllosomas of *P. cygnus*. Siphonophores and other larger and less actively swimming zooplankton might provide an easy prey target for the fragile phyllosomas, which have poor swimming abilities (O'Rourke et al. 2015). Once attached to the prey, the phyllosoma have a large and readily digestible biomass while also eliminating energy expenditure for further predation and vertical migration (Wang et al. 2014a,b). However, availability of siphonophores was limited in the waters we studied (Sawström et al. 2014), and the preferred prey of phyllosomas remain chaetognaths and crustacean zooplankton (Saunders et al. 2012). It was these latter organisms, not the salps and siphonophores, which showed the clearest interannual covariation in isotopic signature with the phyllosomas.

An abundance of dinoflagellate fatty acid markers characterizes the markedly higher quantities of stored lipid found in phyllosomas in CCEs, vs. those WCEs, which, in contrast, are characterized by diatom fatty acid markers (Wang et al. 2014b, 2015). This supports our findings that it is the differently structured phytoplankton communities in the CCEs and WCEs that determine their different nutritional value to zooplankton, and eventually to phyllosoma. The high dinoflagellate marker has also been found to strongly characterize migrating and settling pueruli, as well as successfully settled juveniles (Phillips et al. 2006; Limbourn and Nichols 2009) suggesting that CCEs may have a disproportionate contribution to larval success and subsequent postlarval settlement into the western rock lobster population.

References

- Assmy, P., and others. 2013. Thick-shelled, grazer-protected diatoms decouple ocean carbon and silicon cycles in the iron-limited Antarctic Circumpolar Current. *Proceedings of the National Academy of Sciences* www.pnas.org/cgi/doi/10.1073/pnas.1309345110
- Behrenfeld, M. J. 2010. Abandoning Sverdrup's critical depth hypothesis on phytoplankton blooms. *Ecology* **91**: 977–989. doi:[10.1890/09-1207.1](https://doi.org/10.1890/09-1207.1)
- Caputi, N. 2008. Impact of the Leeuwin Current on the spatial distribution of the puerulus settlement of the western rock lobster (*Panulirus cygnus*) and implications for the fishery of Western Australia. *Fish. Oceanogr.* **17**: 147–152. doi:[10.1111/j.1365-2419.2008.00471.x](https://doi.org/10.1111/j.1365-2419.2008.00471.x)
- Chelton, D. B., M. G. Schlax, and R. M. Samelson. 2011. Global observations of nonlinear mesoscale eddies. *Prog. Oceanogr.* **91**: 167–216. doi:[10.1016/j.pocan.2011.01.002](https://doi.org/10.1016/j.pocan.2011.01.002)

- Cresswell, G., and D. Griffin. 2004. The Leeuwin Current, eddies and sub-Antarctic waters off South-Western Australia. *Mar. Freshw. Res.* **55**: 267–276. doi:[10.1071/MF03115](https://doi.org/10.1071/MF03115)
- Cushing, D. H. 1989. A difference in structure between ecosystems in strongly stratified waters and in those that are only weakly stratified. *J. Plankton Res.* **11**: 1–13. doi:[10.1093/plankt/11.1.1](https://doi.org/10.1093/plankt/11.1.1)
- De Boyer Montégut, C., G. Madec, A. S. Fischer, A. Lazar, and D. Iudicone. 2004. Mixed layer depth over the global ocean: An examination of profile data and a profile-based climatology. *J. Geophys. Res. Oceans* **109**: C12003. doi:[10.1029/2004JC002378](https://doi.org/10.1029/2004JC002378)
- Dufois, F., N. J. Hardman-Mountford, J. Greenwood, A. J. Richardson, M. Feng, and R. J. Matear. 2016. Anticyclonic eddies are more productive than cyclonic eddies in subtropical gyres because of winter mixing. *Sci. Adv.* **2**: e1600282. doi:[10.1126/sciadv.1600282](https://doi.org/10.1126/sciadv.1600282)
- Feng, M., G. Meyers, A. Pearce, and S. Wijffels. 2003. Annual and interannual variations of the Leeuwin Current at 32S. *J. Geophys. Res.* **108**: 3355. doi:[10.1029/2002JC001763](https://doi.org/10.1029/2002JC001763).
- Feng, M., L. Majewski, C. Fandry, and A. Waite. 2007. Characteristics of two counter-rotating eddies in the Leeuwin Current system off the Western Australian coast. *Deep-Sea Res. Part II Top. Stud. Oceanogr.* **54**: 961–980.
- Feng, M., A. M. Waite, and P. A. Thompson. 2009. Climate variability and ocean production in the Leeuwin Current system of the west coast of Western Australia. *J. R. Soc. West. Aust.* **92**: 67–81.
- Finkel, Z. V., M. J. Follows, and A. J. Irwin. 2016a. Size-scaling of macromolecules and chemical energy content in the eukaryotic microalgae. *J. Plankton Res.* **38**: 1151–1162.
- Finkel, Z. V., M. J. Follows, J. D. Liefer, C. M. Brown, I. Benner, and A. J. Irwin. 2016b. Phylogenetic diversity in the macromolecular composition of microalgae. *PLoS One* **11**: e0155977.
- Fox, J., and S. Weisberg. 2010. *An R companion to applied regression*. Sage.
- Friedrichs, L., M. Hoernig, L. Schulze, A. Bertram, S. Jansen, and C. Hamm. 2013. Size and biomechanic properties of diatom frustules influence food uptake by copepods. *Mar. Ecol. Prog. Ser.* **481**: 41–51. doi:[10.3354/meps10227](https://doi.org/10.3354/meps10227).
- Greenwood, J. E., M. Feng, and A. M. Waite. 2007. A one-dimensional simulation of biological production in two contrasting mesoscale eddies in the south eastern Indian Ocean. *Deep-Sea Res. Part II Top. Stud. Oceanogr.* **54**: 1029–1044. doi:[10.1016/j.dsr2.2006.10.004](https://doi.org/10.1016/j.dsr2.2006.10.004)
- Hannides, C. C., B. N. Bopp, D. A. Choy, and J. C. Drazen. 2013. Midwater zooplankton and suspended particle dynamics in the North Pacific Subtropical Gyre: A stable isotope perspective. *Limnol. Oceanogr.* **58**: 1931–1946. doi:[10.4319/lo.2013.58.6.1931](https://doi.org/10.4319/lo.2013.58.6.1931)
- Hanson, C. E., C. B. Pattiaratchi, and A. M. Waite. 2005. Sporadic upwelling on a downwelling coast: Phytoplankton responses to spatially variable nutrient dynamics off the Gascoyne region of Western Australia. *Cont. Shelf Res.* **25**: 1561–1582. doi:[10.1016/j.csr.2005.04.003](https://doi.org/10.1016/j.csr.2005.04.003)
- Hanson, C. E., S. Pesant, A. M. Waite, and C. B. Pattiaratchi. 2007. Assessing the magnitude and significance of deep chlorophyll maxima of the coastal eastern Indian Ocean. *Deep-Sea Res. Part II Top. Stud. Oceanogr.* **54**: 884–901. doi:[10.1016/j.dsr2.2006.08.021](https://doi.org/10.1016/j.dsr2.2006.08.021)
- Hitchcock, G. L. 1982. A comparative study of the size-dependent organic composition of marine diatoms and dinoflagellates. *J. Plankton Res.* **4**: 363–377. doi:[10.1093/plankt/4.2.363](https://doi.org/10.1093/plankt/4.2.363)
- Högländer, H., U. Larsson, and S. Hajdu. 2004. Vertical distribution and settling of spring phytoplankton in the offshore NW Baltic Sea proper. *Mar. Ecol. Prog. Ser.* **283**: 15–27. doi:[10.3354/meps283015](https://doi.org/10.3354/meps283015)
- Hötzel, G., and R. Croome. 1999. *A phytoplankton methods manual for Australian freshwaters*. Land and Water Resources Research and Development Corporation.
- Jones, R. H., and K. J. Flynn. 2005. Nutritional status and diet composition affect the value of diatoms as copepod prey. *Science* **307**: 1457–1459. doi:[10.1126/science.1107767](https://doi.org/10.1126/science.1107767)
- Limbourn, A. J., and P. D. Nichols. 2009. Lipid, fatty acid and protein content of late larval to early juvenile stages of the western rock lobster, *Panulirus cygnus*. *Comp. Biochem. Physiol. B Biochem. Mol. Biol.* **152**: 292–298. doi:[10.1016/j.cbpb.2008.12.009](https://doi.org/10.1016/j.cbpb.2008.12.009)
- Long, J. S., and L. H. Ervin. 2000. Using heteroscedasticity consistent standard errors in the linear regression model. *Am. Stat.* **54**: 217–224.
- Mansour, M. P., J. K. Volkman, and S. I. Blackburn. 2003. The effect of growth phase on the lipid class, fatty acid and sterol composition in the marine dinoflagellate, *Gymnodinium* sp. in batch culture. *Phytochemistry* **63**: 145–153.
- McCue, M. D. 2012. *Comparative physiology of fasting, starvation, and food limitation*. Springer.
- Mills, C. E. 1995. Medusae, siphonophores, and ctenophores as planktivorous predators in changing global ecosystems. *ICES J. Mar. Sci.* **52**: 575–581. doi:[10.1016/1054-3139\(95\)80072-7](https://doi.org/10.1016/1054-3139(95)80072-7)
- Montoya, J. P. 2008. Nitrogen stable isotopes in marine environments. In D. G. Capone, E. J. Carpenter, M. R. Mulholland, and D. A. Bronk [eds.], *Nitrogen in the marine environment*. Academic Press. pp. 1277–1302. doi:[10.1016/B978-0-12-372522-6.00029-3](https://doi.org/10.1016/B978-0-12-372522-6.00029-3)
- Morris, I., C. M. Yentsch, and C. S. Yentsch. 1971. Relationship between light carbon dioxide fixation and dark carbon dioxide fixation by marine algae. *Limnol. Oceanogr.* **16**: 854–857. doi:[10.4319/lo.1971.16.6.0854](https://doi.org/10.4319/lo.1971.16.6.0854)
- Omand, M. M., E. A. D'Asaro, C. M. Lee, M. J. Perry, N. Briggs, I. Cetinic, and A. Mahadevan. 2015. Eddy-driven subduction exports particulate organic carbon from the spring bloom. *Science* **348**: 222–225. doi:[10.1126/science.1260062](https://doi.org/10.1126/science.1260062)
- O'Rourke, R., and others. 2012. Determining the diet of larvae of western rock lobster (*Panulirus cygnus*) using high-throughput

- DNA sequencing techniques. *PLoS One* **7**: e42757. doi:[10.1371/journal.pone.0042757](https://doi.org/10.1371/journal.pone.0042757)
- O'Rourke, R., A. G. Jeffs, Q. P. Fitzgibbon, S. Chow, and S. Lavery. 2013. Extracting DNA from whole organism homogenates and the risk of false positives in PCR based diet studies: A case study using spiny lobster larvae. *J. Exp. Mar. Biol. Ecol.* **441**: 1–6. doi:[10.1016/j.jembe.2013.01.003](https://doi.org/10.1016/j.jembe.2013.01.003)
- O'Rourke, R., A. G. Jeffs, M. Wang, A. M. Waite, L. E. Beckley, and S. D. Lavery. 2015. Spinning in different directions: Western rock lobster larval condition varies with eddy polarity, but does their diet? *J. Plankton Res.* **37**: 542–553. doi:[10.1093/plankt/fbv026](https://doi.org/10.1093/plankt/fbv026)
- O'Rourke, R., S. D. Lavery, M. Wang, R. Gallego, A. M. Waite, L. E. Beckley, P. Thompson, and A. G. Jeffs. 2015. Phyllosomata associated with large gelatinous zooplankton: Hitching rides and stealing bites. *ICES J. Mar. Sci.* **72**: i124–i127. doi:[10.1093/icesjms/fsu163](https://doi.org/10.1093/icesjms/fsu163)
- Parsons, T., Y. Maita, and C. Lalli. 1984. A manual of chemical and biological methods for seawater analysis. Pergamon.
- Paterson, H. L., M. Feng, A. M. Waite, D. Gomis, L. E. Beckley, D. Holliday, and P. A. Thompson. 2008. Physical and chemical signatures of a developing anticyclonic eddy in the Leeuwin Current, eastern Indian Ocean. *J. Geophys. Res. Oceans* **113**: C07049. doi:[10.1029/2007JC004707](https://doi.org/10.1029/2007JC004707)
- Paul, D., G. Skrzypek, and I. Forizs. 2007. Normalization of measured stable isotopic compositions to isotope reference scales—a review. *Rapid Commun. Mass Spectrom.* **21**: 3006–3014. doi:[10.1002/rcm.3185](https://doi.org/10.1002/rcm.3185)
- Phillips, B. F., A. G. Jeffs, R. Melville-Smith, C. F. Chubb, M. M. Nelson, and P. D. Nichols. 2006. Changes in lipid and fatty acid composition of late larval and puerulus stages of the spiny lobster (*Panulirus cygnus*) across the continental shelf of Western Australia. *Comp. Biochem. Physiol. B Biochem. Mol. Biol.* **143**: 219–228. doi:[10.1016/j.cbpb.2005.11.009](https://doi.org/10.1016/j.cbpb.2005.11.009)
- Pidcock, R. E., A. P. Martin, S. C. Painter, A. E. Allen, A. Forryan, M. Stinchcombe, and D. A. Smeed. 2016. Quantifying mesoscale-driven nitrate supply: A case study. *Global Biogeochem. Cycles* **30**: 1206–1223. doi:[10.1002/2016GB005383](https://doi.org/10.1002/2016GB005383)
- Purcell, J. E. 1997. Pelagic cnidarians and ctenophores as predators: Selective predation, feeding rates, and effects on prey populations. *Ann. Inst. Océanogr.* **73**: 125–137.
- R Core Team. 2013. R development core team. *R. A. Lang. Environ. Stat. Comput.* **55**: 275–286.
- Raes, E. J., P. A. Thompson, A. S. McInnes, H. M. Nguyen, N. Hardman-Mountford, and A. M. Waite. 2015. Sources of new nitrogen in the Indian Ocean. *Global Biogeochem. Cycles* **29**: 1283–1297. doi:[10.1002/2015GB005194](https://doi.org/10.1002/2015GB005194)
- Rossi, V., M. Feng, C. Pattiaratchi, M. Roughan, and A. M. Waite. 2013. On the factors influencing the development of sporadic upwelling in the Leeuwin Current system. *J. Geophys. Res. Oceans* **118**: 3608–3621. doi:[10.1002/jgrc.20242](https://doi.org/10.1002/jgrc.20242)
- Rousseaux, C. S. G., R. Lowe, M. Feng, A. M. Waite, and P. A. Thompson. 2012. The role of the Leeuwin Current and mixed layer depth on the autumn phytoplankton bloom off Ningaloo Reef, Western Australia. *Cont. Shelf Res.* **32**: 22–35. doi:[10.1016/j.csr.2011.10.010](https://doi.org/10.1016/j.csr.2011.10.010)
- Sato, M., H. Sasaki, and M. Fukuchi. 2002. Stable isotopic compositions of overwintering copepods in the arctic and sub-arctic waters and implications to the feeding history. *J. Mar. Syst.* **38**: 165–174. doi:[10.1016/S0924-7963\(02\)00175-6](https://doi.org/10.1016/S0924-7963(02)00175-6)
- Saunders, M. I., P. A. Thompson, A. G. Jeffs, C. Saewstroem, N. Sachlikidis, L. E. Beckley, and A. M. Waite. 2012. Fussy feeders: Phyllosoma larvae of the Western Rocklobster (*Panulirus cygnus*) demonstrate prey preference. *PLoS One* **7**: e36580. doi:[10.1371/journal.pone.0036580](https://doi.org/10.1371/journal.pone.0036580)
- Säwström, C., L. E. Beckley, M. I. Saunders, P. A. Thompson, and A. M. Waite. 2014. The zooplankton prey field for rock lobster phyllosoma larvae in relation to oceanographic features of the south-eastern Indian Ocean. *J. Plankton Res.* **36**: 1003–1016. doi:[10.1093/plankt/fbu019](https://doi.org/10.1093/plankt/fbu019)
- Skrzypek, G., R. Sadler, and D. Paul. 2010. Error propagation in normalization of stable isotope data: A Monte Carlo analysis. *Rapid Commun. Mass Spectrom.* **24**: 2697–2705. doi:[10.1002/rcm.4684](https://doi.org/10.1002/rcm.4684)
- Stoecker, D. K., and J. M. Capuzzo. 1990. Predation on protozoa: Its importance to zooplankton. *J. Plankton Res.* **12**: 891–908. doi:[10.1093/plankt/12.5.891](https://doi.org/10.1093/plankt/12.5.891)
- Strzelecki, J., J. Koslow, and A. Waite. 2007. Comparison of mesozooplankton communities from a pair of warm-and cold-core eddies off the coast of Western Australia. *Deep-Sea Res. Part II Top. Stud. Oceanogr.* **54**: 1103–1112. doi:[10.1016/j.dsr2.2007.02.004](https://doi.org/10.1016/j.dsr2.2007.02.004)
- Thompson, P. A., S. Pesant, and A. M. Waite. 2007. Contrasting the vertical differences in the phytoplankton biology of a dipole pair of eddies in the south-eastern Indian Ocean. *Deep-Sea Res. Part II Top. Stud. Oceanogr.* **54**: 1003–1028. doi:[10.1016/j.dsr2.2006.12.009](https://doi.org/10.1016/j.dsr2.2006.12.009)
- Waite, A., P. K. Bienfang, and P. J. Harrison. 1992. Spring bloom sedimentation in a sub-arctic ecosystem: 1. Nutrient sensitivity. *Mar. Biol.* **114**: 119–129.
- Waite, A. M., B. A. Muhling, C. M. Holl, L. E. Beckley, J. P. Montoya, J. Strzelecki, P. A. Thompson, and S. Pesant. 2007a. Food web structure in two counter-rotating eddies based on delta N-15 and delta C-13 isotopic analyses. *Deep-Sea Res. Part II Top. Stud. Oceanogr.* **54**: 1055–1075.
- Waite, A. M., S. Pesant, D. A. Griffin, P. A. Thompson, and C. M. Holl. 2007b. Oceanography, primary production and dissolved inorganic nitrogen uptake in two Leeuwin Current eddies. *Deep-Sea Res. Part II Top. Stud. Oceanogr.* **54**: 981–1002.
- Waite, A. M., and others. 2016a. The wine glass effect shapes particle export to the deep ocean in mesoscale eddies. *Geophys. Res. Lett.* **43**: 9791–9800. doi:[10.1002/2015GL066463](https://doi.org/10.1002/2015GL066463)
- Waite, A. M., and others. 2016b. Cross-shelf transport, oxygen depletion, and nitrate release within a forming mesoscale eddy in the eastern Indian Ocean. *Limnol. Oceanogr.* **61**: 103–121.
- Wang, M., R. O'Rourke, S. D. Nodder, and A. G. Jeffs. 2014a. Nutritional composition of potential zooplankton prey of

- the spiny lobster phyllosoma (*Jasus edwardsii*). Mar. Freshw. Res. **65**: 337–349.
- Wang, M., R. O'Rorke, A. M. Waite, L. E. Beckley, P. Thompson, and A. G. Jeffs. 2014b. Fatty acid profiles of phyllosoma larvae of western rock lobster (*Panulirus cygnus*) in cyclonic and anticyclonic eddies of the Leeuwin Current off Western Australia. Prog. Oceanogr. **122**: 153–162.
- Wang, M., R. O'Rorke, A. M. Waite, L. E. Beckley, P. Thompson, and A. G. Jeffs. 2015. Condition of larvae of western rock lobster (*Panulirus cygnus*) in cyclonic and anticyclonic eddies of the Leeuwin Current off Western Australia. Mar. Freshw. Res. **66**: 1158–1167. doi:[10.1071/MF14121](https://doi.org/10.1071/MF14121)
- Waser, N. A. D., W. G. Harrison, E. J. H. Head, B. Nielsen, V. A. Lutz, and S. E. Calvert. 2000. Geographic variations in the nitrogen isotope composition of surface particulate nitrogen and new production across the North Atlantic Ocean. Deep-Sea Res. Part I Oceanogr. Res. Pap. **47**: 1207–1226.
- Wasmund, N., M. Voss, and K. Lochte. 2001. Evidence of nitrogen fixation by non-heterocystous cyanobacteria in the Baltic Sea and re-calculation of a budget of nitrogen fixation. Mar. Ecol. Prog. Ser. **214**: 1–14. doi:[10.3354/meps214001](https://doi.org/10.3354/meps214001)
- Wright, S. W., S. W. Jeffrey, R. F. C. Mantoura, C. A. Llewellyn, T. Bjornland, D. Repeta, and N. Welschmeyer. 1991. Improved HPLC method for the analysis of chlorophylls and carotenoids

from marine phytoplankton. Mar. Ecol. Prog. Ser. **77**: 183–196. doi:[10.3354/meps077183](https://doi.org/10.3354/meps077183)

Acknowledgments

Many thanks to Kate Patterson for patient assistance with Figs. 1–3. We are grateful to Amala Mahadevan for important discussions regarding physical mechanisms driving nitrate supply in mesoscale eddies, and to Zoe Finkel for discussions regarding phytoplankton nutritional value. The RV *Southern Surveyor* was provided by the Australian Marine National Facility under Grants SS08-2003, SS05-2006, SS05-2010, and SS04-2011. This project was funded by a grant from the Fisheries Research and Development Corporation of Australia under FRDC project number: 2010/047. The research is a contribution to the Worldwide Universities Network project “Ocean eddies in a changing climate: Understanding the impact of coastal climates and fisheries production.” We thank all the people who assisted in sample collection and the captains and crew of the RV *Southern Surveyor*.

Conflict of Interest

None declared.

Submitted 21 August 2017

Revised 01 July 2018

Accepted 03 April 2019

Associate editor: Craig Stevens